

Material tests for the characterisation of replicated solid clay brick masonry

Licciardello, Lucia; Esposito, Rita

Publication date

2019

Document Version

Final published version

Citation (APA)

Licciardello, L., & Esposito, R. (2019). *Material tests for the characterisation of replicated solid clay brick masonry*. Delft University of Technology.

Important note

To cite this publication, please use the final published version (if applicable).
Please check the document version above.

Copyright

Other than for strictly personal use, it is not permitted to download, forward or distribute the text or part of it, without the consent of the author(s) and/or copyright holder(s), unless the work is under an open content license such as Creative Commons.

Takedown policy

Please contact us and provide details if you believe this document breaches copyrights.
We will remove access to the work immediately and investigate your claim.

<i>Project number</i>	CM1B04
<i>File reference</i>	CM1B04-WPC-2.3
<i>Date</i>	7 October 2019
<i>Corresponding author</i>	Rita Esposito (r.esposito@tudelft.nl)

TU Delft Large-scale testing campaign 2019

MATERIAL TESTS FOR THE CHARACTERISATION OF REPLICATED SOLID CLAY BRICK MASONRY

Authors: Lucia Licciardello, Rita Esposito

Cite as: Licciardello, L and Esposito, R. Material tests for the characterisation of replicated solid clay brick masonry. Report No. CM1B04-WPC-2.3, 7 October 2019. Delft University of Technology.

This document is made available via the website ‘Structural Response to Earthquakes’ and the TU Delft repository. While citing, please verify if there are recent updates of this research in the form of scientific papers.

All rights reserved. No part of this publication may be reproduced, stored in a retrieval system of any nature, or transmitted, in any form or by any means, electronic, mechanical, photocopying, recording or otherwise, without the prior written permission of TU Delft.

TU Delft and those who have contributed to this publication did exercise the greatest care in putting together this publication. This report will be available as-is, and TU Delft makes no representations of warranties of any kind concerning this Report. This includes, without limitation, fitness for a particular purpose, non-infringement, absence of latent or other defects, accuracy, or the presence or absence of errors, whether or not discoverable. Except to the extent required by applicable law, in no event will TU Delft be liable for on any legal theory for any special, incidental consequential, punitive or exemplary damages arising out of the use of this report.

This research work was funded by NAM Structural Upgrading stream.

Table of Contents

1	Introduction.....	5
2	Nomenclature	6
2.1	Symbols	6
2.2	Abbreviations.....	8
3	Construction of the samples	9
4	Flexural and compressive strength of mortar.....	10
4.1	Testing procedure.....	10
4.2	Experimental results.....	10
5	Density of masonry.....	14
6	Compression properties of masonry	16
6.1	Testing procedure.....	16
6.2	Experimental results.....	17
7	Bond strength of masonry	25
7.1	Testing procedure.....	25
7.2	Experimental results.....	26
8	Shear strength of masonry	31
8.1	Testing procedure.....	31
8.2	Experimental results.....	32
9	Summary and properties overview	37
	References	40
	Appendix A.....	41

1 Introduction

In support to the strengthening of unreinforced masonry buildings in the Groningen area, a combined experimental and numerical study of retrofitting measures was carried out at TU Delft as part of the 2019 project “Structural upgrading of masonry structures in the Groningen area”. The project consists of four main work packages:

- WP1: Study of the as-built and retrofitted behaviour of connections for the creation of a database;
- WP2: Characterisation of the as-built and retrofitted behaviour of connections between masonry wall and timber floor;
- WP3: Numerical study on retrofitting measures for low-rise URM buildings;
- WPC: Companion material tests.

This report provides the final results of WPC, concerning the companion material tests for masonry, that support the experimental research on the connection tests performed in WP2 [1]. The experimental campaign focuses on the use on solid clay brick masonry. The tests have been performed twice following the different testing phases of WP2: the companion material tests performed on specimens built in March 2019 refer to the first testing phase of WP2, while the companion material tests performed on specimens built in May 2019 refer to the second testing phase of WP2.

In WPC only selected material tests have been performed, because an extensive characterisation of the solid clay brick masonry was provided in a previous experimental campaign carried out in 2016 [2]; furthermore the same material was used in Ref. [3]-[4]. The bricks and mortar used in this and previous experimental campaign belong to a single production batch; the same construction procedure has been adopted. The material was originally selected to replicate properties of solid clay brick masonry as obtained by tests on specimens extracted from existing buildings in Groningen [5]. A complete overview of this selection can be found in Ref. [6]. The experimental results presented in this document are in line with results from previous experimental campaigns.

The material properties obtained within this testing campaign can be used as input for analytical and numerical models. By using well-designed displacement-control testing set-ups, the compression, bending and shear properties of masonry specimens were measured, indicating strength, stiffness and softening post-peak behaviour of solid clay brick masonry. A set of required input masonry properties pursued within this research is listed in Table 1. Section 2 lists the adopted nomenclature. Section 3 provides information on the construction of the specimens. The flexural and compressive strength of mortar is provided in Section 4. The density of masonry is reported in Section 5. The compression, bending and shear properties of single wythe masonry are reported from Section 6 to Section 8. An overview of the obtained material properties is reported in Section 9 including data from previous experimental campaigns.

Table 1 – Overview of tests and material properties reported in this document.

	Type of test	Material property
Mortar	Compression test	Compressive strength of masonry mortar
	Flexural test	Flexural strength of masonry mortar
Masonry	Vertical Compression test	Compressive strength Young's modulus Fracture energy in compression Poisson ratio Stress-strain relationship in compression (pre- and post-peak)
	Shear-compression test	Initial and residual shear strength Initial and residual shear friction coefficient Mode-II fracture energy Shear stress vs. shear displacement relationship (pre- and post-peak)
	Bond wrench test	Flexural bond strength

2 Nomenclature

2.1 Symbols

This report adopts mainly the nomenclature used in Eurocode 6 [7]. In addition, symbols used in the codes for testing are adopted.

α	Masonry (bed joint) angle of internal friction
α_{res}	Masonry (bed joint) residual angle of internal friction
ν	Poisson ratio of masonry
μ	Masonry (bed joint) shear strength coefficient
μ_{res}	Masonry (bed joint) residual shear strength coefficient
ε_p	Strain associated with peak strength in vertical compression test
$\varepsilon_{p,h}$	Strain associated with peak strength in horizontal compression test
d_1	Distance between bearing supports
d_2	Distance between loading supports
d_3	Distance between the loading and bearing supports (four-point bending test)
f_m	Compressive strength of masonry mortar
f_{m_t}	Flexural strength of masonry mortar
f'_m	Compressive strength of masonry in the direction perpendicular to the bed joints
$f'_{m,h}$	Compressive strength of masonry in the direction parallel to the bed joints
f_p	Applied lateral pre-compression stress
f_{x1}	Masonry flexural strength with the moment vector parallel to the bed joints and in the plane of the wall, which generates a plane of failure parallel to the bed joints
f_{x2}	Masonry flexural strength with the moment vector orthogonal to the bed joints and in the plane of the wall, which generates a plane of failure perpendicular to the bed joints
f_{x3}	Masonry flexural strength with the moment vector orthogonal to the plane of the wall
f_{v0}	Masonry (bed joint) initial shear strength
$f_{v0,res}$	Masonry (bed joint) residual initial shear strength
f_w	Masonry uniaxial bond strength between the masonry unit and the mortar
l_j	Length of the mortar bed joint in a masonry specimens
l_m	Length of the mortar specimen
l_s	Length of the masonry specimen as built
l_p	Length of the loading plate for compression tests on mortar specimens
l_u	Length of the masonry unit as used in the construction of masonry
h_m	Height of the mortar specimen
h_s	Height of the masonry specimen as built
h_u	Height of the masonry unit as used in the construction
t_s	Thickness of the masonry specimen as built

t_m	Thickness of the mortar specimen
t_u	Thickness of the masonry unit as used in the construction of masonry
v_{el}	Vertical displacement corresponding to the load F_{el}
A_s	Cross sectional area of the specimen parallel to the bed joints (shear test)
E_b	Chord elastic modulus of stacked masonry unit subjected to compression load
E_1	Secant elastic modulus of masonry subject to a compressive loading perpendicular to the bed joints, evaluated at 1/3 of the maximum stress
E_2	Secant elastic modulus of masonry subject to a compressive loading perpendicular to the bed joints, evaluated at 1/10 of the maximum stress
E_3	Chord elastic modulus of masonry subject to a compressive loading perpendicular to the bed joints, evaluated at between 1/10 and 1/3 of the maximum stress
$E_{1,h}$	Secant elastic modulus of masonry subject to a compressive loading parallel to the bed joints, evaluated at 1/3 of the maximum stress
$E_{2,h}$	Secant elastic modulus of masonry subject to a compressive loading parallel to the bed joints, evaluated at 1/10 of the maximum stress
$E_{3,h}$	Chord elastic modulus of masonry subject to a compressive loading parallel to the bed joints, evaluated at between 1/10 and 1/3 of the maximum stress
E_{bt}	Chord elastic modulus of masonry unit subjected to the bending load
E_{fx1}	Chord elastic modulus of masonry in bending parallel to the bed joints evaluated between 1/10 and 1/3 of the maximum force
E_{fx2}	Chord elastic modulus of masonry in bending perpendicular to the bed joints evaluated between 1/10 and 1/3 of the maximum force
E_{fx3}	Chord elastic modulus of masonry subjected to bending load with the moment vector orthogonal to the plane of the wall evaluated between 1/10 and 1/3 of the maximum force
F_1	Applied vertical load (bond-wrench test)
F_2	Vertical load due to the weight of the top clamping system (bond-wrench test)
F_3	Vertical load due to the top masonry unit (bond-wrench test)
F_{el}	Selected vertical load value in the linear elastic stage (flexural test of masonry unit)
F_{max}	Maximum vertical load
F_p	Applied lateral pre-compression force (shear test)
G_{f-c}	Fracture energy in compression for loading perpendicular to the bed joints
$G_{f-c,h}$	Fracture energy in compression for loading parallel to the bed joints
G_{fII}	Mode II fracture energy in shear
G_{fx1}	Fracture energy obtained from bending tests with the moment vector parallel to the bed joints and in the plane of the wall, which generates a plane of failure parallel to the bed joints
G_{fx2}	Fracture energy obtained from bending tests with the moment vector orthogonal to the bed joints and in the plane of the wall, which generates a plane of failure perpendicular to the bed joints
G_{fx3}	Fracture energy obtained from bending tests with the moment vector orthogonal to the plane of the wall
G_{fw}	Fracture energy obtained with computer controlled bond wrench test
M_{max}	Maximum bending moment
W	Section modulus
I	Moment of inertia of the masonry unit along the cross-section

2.2 Abbreviations

Avg.	Average
C.o.V.	Coefficient of variation
CS	Calcium silicate
LVDT	Linear variable differential transformer
St. dev.	Standard deviation

3 Construction of the samples

The masonry specimens were built in the Stevin II laboratory at Delft University of Technology. The masonry was made of clay bricks and cement based mortar. The declarations of performance of the materials are reported in Appendix A.

Figure 1 shows the adopted masonry unit. The dimensions are defined considering the orientation of the masonry unit as used in the construction of the masonry. This definition is consistently adopted in this report despite the position of the specimen in the test set-up. A similar consideration is applied to describe the dimensions of masonry specimens.

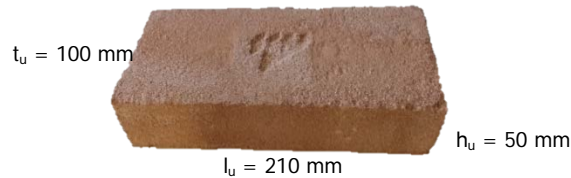


Figure 1 – Mean dimensions of the clay bricks.

In order to ensure quality control, the construction followed the prescription as reported in the construction protocol [8]:

- The bags of mortar mix were stored dry and separated from the soil;
- The mortar mix was used within 18 months after production;
- The mortar was mixed with clean water;
- The mortar was prepared using a fixed water content;
- The flow of the mortar was determined in agreement with EN 1015-3:1999 [9].
- At least three samples of mortar (size 160x40x40-mm) were made at every start of the day during construction of masonry for testing the properties. The samples were tested under flexural and compressive loading in agreement with EN 1015-11:1999 [10];
- The mortar was prepared and used between 5 and 25 degrees;
- The mortar was used within 2 hours after preparation;
- No additives were mixed after preparation of the mortar;
- Bricks were covered against moisture;
- Bricks were clean before use;
- Bricks were not wetted before use;

The mortar was prepared with fixed water content per bag of mix (25 kg): 3.7 l/bag for clay brick masonry.

4 Flexural and compressive strength of mortar

During the masonry construction, mortar samples were collected and cast in moulds to be tested for the flexural and compressive strength in agreement with EN 1015-11:1999 [10]. The consistency of the mortar was determined in accordance with EN 1015-3:1999 [9].

4.1 Testing procedure

During each day of construction, at least three mortar specimens having a length of $l_m = 160$ mm, a height of $h_m = 40$ mm and thickness of $t_m = 40$ mm were collected. The samples were stored in controlled conditions. The first two days they were placed in a fog room ($T = 20 \pm 2$ °C, $RH = 95 \pm 5\%$) with the moulds. After two days, they were un moulded and kept for other five days in the fog room. Eventually, they were placed in a conditioning room with a temperature of 20 ± 2 °C and a relative humidity of 50 ± 5 % until testing. The test was performed after at least 28 days from construction.

The flexural strength was determined by three-point bending test (Figure 2a). The test set-up is composed by two steel bearing rollers having a diameter of 10 ± 0.5 mm and spaced $d_1 = 100 \pm 0.5$ mm. A third roller is centrally placed on top of the sample to apply the load.

The compression test was performed on the broken pieces obtained from the flexural test, which have at least a length of 40 mm. The specimen is placed between two steel plates with a length of $l_p = 40$ mm. For the interpretation of the results the specimens considered to be 40x40x40-mm (Figure 2b).

For both test, the load was applied without shock at a uniform rate so that failure occurred within a period of 30 to 90 s. The maximum load was recorded.



Figure 2 – Test on masonry mortar specimens: (a) three-point bending test; (b) compression test.

4.2 Experimental results

The flexural strength f_{mt} of the mortar was calculated as [10]:

$$f_{mt} = \frac{3 F_{max} d_1}{2 t_m h_m^2} \quad (1)$$

where F_{max} is the maximum load, d_1 is the distance between the supports ($100 \text{ mm} \pm 0.5 \text{ mm}$), h_m is the height of the mortar specimen (40 mm) and t_m is the thickness of the mortar specimen (40mm).

The compressive strength f_m of the mortar was calculated as [10]:

$$f_m = \frac{F_{max}}{t_m l_p} \quad (2)$$

where F_{max} is the maximum load, t_m is the thickness of the mortar specimen (40 mm) and l_p is the length of the loading plate (40 mm).

During the masonry construction, the slump test was performed after the preparation of every batch of mortar. The diameter of the cone was obtained in agreement with the slump test described in EN 1015-3:1999 [9]. The measured diameter varied between 170 to 196 mm (Table 2 and Table 3).

The flexural and compression tests on the hardened mortar were performed after 28 days. Table 4 list the results for the three-point bending tests and compression tests for the construction period of March 2019 and May 2019, respectively. Three-point bending tests were performed on 12 mortar bars and compressive tests were conducted on 24 broken pieces obtained from the flexural tests. The values of the flexural strength and compressive strength for each batch are obtained from performing tests on the three mortar bars. These values are obtained considering the average of all the tested specimens. No significant differences for the mortar properties are observed between the two construction periods: the flexural strength is 2.16 MPa and 1.92 MPa and the compressive strength is 4.65 MPa and 5.04MPa for the first and the second construction period, respectively.

Table 2 – Consistency of mortar construction period March 2019.

Date of construction	Number of batch	Companion sample	Flow (mm)
28-02-2019	1	Masonry-timber connection sample	173
	2		181
	3		170
	4		183
	5		183
01-03-2019	6	Masonry-timber connection sample MAT-31 MAT-36 MAT-35	172
	7		183
	8		180
	9		173
	10		169
Average			177

Table 3 – Consistency of mortar construction period May 2019.

Date of construction	Number of batch	Companion sample	Flow (mm)
27-5-2019	1	Masonry-timber connection sample MAT-31	177
	2		192
	3		196
28-5-2019	1	Masonry-timber connection sample MAT-36 MAT-35	184
	2		186
Average			187

Table 4 – Flexural and compressive strength of mortar from construction period March 2019.

Date of construction	Batch	Density	Flexural strength	Compressive strength
		(kg/m ³)	f_{mt} (MPa)	f_m (MPa)
28-02-2019	1	1660	2.22	4.62
				4.76
		1699	2.43	5.74
				4.96
		1641	1.93	5.09
				4.97
28-02-2019	5	1738	1.51	4.62
				3.98
		1758	2.51	4.21
				4.68
		1758	1.84	5.41
				4.87
01-03-2019	6	1934	2.51	4.28
				4.52
		1895	2.14	4.83
				4.59
		1933	2.43	4.12
				5.08
01-03-2019	9	1738	-	4.20
				4.39
		1738	0.55	4.64
				4.50
		1738	-	4.45
				4.06
Average		1769	2.16	4.65
Standard deviation		95	0.35	0.42
Coefficient of variation		0.05	0.16	0.09

*The specimen was broken before the flexural test; Only compression properties were tested.

Table 5 - Flexural and compressive strength of mortar from construction period May 2019

Date of construction	Batch	Density (kg/m ³)	Flexural strength f_{mt} (MPa)	Compressive strength f_m (MPa)
27-5-2019	1	1719	1.77	5.34
				5.11
		1758	1.95	5.30
				5.10
		1738	1.83	5.30
				5.60
27-5-2019	3	1758	2.22	5.63
				5.82
		1738	1.99	4.83
				5.43
		1738	2.24	4.38
				4.91
28-5-2019	4	1602	1.80	4.16
				3.32
		1641	2.18	3.37
				4.91
		1699	1.12	5.76
				5.93
28-5-2019	5	1699	1.86	5.08
				5.43
		1719	1.99	5.23
				4.91
		1719	2.08	5.26
				4.86
Average		1711	1.92	5.04
Standard deviation		47	0.30	0.67
Coefficient of variation		0.03	0.16	0.13

5 Density of masonry

To measure the density of solid clay brick masonry, weight and dimensions of the specimens adopted for the bond wrench test were measured prior to testing. The average value of the density for the solid clay brick masonry is reported as 1618 kg/m³ (Table 6) and 1586 kg/m³ (Table 7) for the first and the second construction period, respectively.

Table 6 – Density of solid clay brick masonry of construction period March 2019.

h_s	L_s	t_s	Weight	Density
mm	mm	mm	kg	kg/m ³
110	210	100	3.71	1606
110	210	100	3.70	1602
110	210	100	3.70	1602
110	210	100	3.73	1615
110	210	100	3.73	1615
110	210	100	3.73	1615
110	210	100	3.75	1623
110	210	100	3.78	1636
110	210	100	3.71	1606
110	210	100	3.82	1654
110	210	100	3.74	1619
110	210	100	3.76	1628
110	210	100	3.79	1641
110	208	100	3.70	1602
110	210	100	3.71	1606
110	210	100	3.73	1615
110	210	100	3.69	1597
110	210	100	3.78	1636
110	210	100	3.77	1632
110	210	100	3.74	1619
Average				1618
Standard Deviation				15
Coefficient of variation				0.01

Table 7 - Density of solid clay brick masonry of construction period May 2019.

h_s	L_s	t_s	Weight	Density
mm	mm	mm	kg	kg/m ³
107	203	100	3.64	1574
112	206	101	3.70	1600
109	205	100	3.69	1597
109	204	100	3.63	1569
109	204	100	3.71	1604
108	205	100	3.63	1571
111	207	100	3.69	1597
112	207	100	3.68	1593
105	205	100	3.61	1561
109	205	100	3.65	1578
111	207	100	3.61	1563
112	207	102	3.69	1597
109	207	100	3.65	1580
107	205	100	3.65	1578
107	204	100	3.65	1580
110	207	102	3.72	1608
107	206	100	3.66	1582
108	206	102	3.64	1574
108	207	100	3.69	1597
111	208	102	3.71	1606
111	206	100	3.72	1610
107	205	101	3.66	1582
108	205	100	3.65	1580
Average				1586
Standard Deviation				15
Coefficient of variation				0.009

6 Compression properties of masonry

The compression strength and elastic modulus of the masonry were determined in agreement with EN 1052-1:1998 [11].

6.1 Testing procedure

The compression strength and elastic modulus of the masonry were determined by applying the load perpendicular to the bed joints.

The dimensions of the specimens and the LVDTs position are shown in Figure 3a.

Four LVDTs (two for each side) were attached to the specimen to register vertical relative displacements over the height of the specimen. They were installed as closely as possible to the surface of the specimen to reduce possible errors caused by rotation of the contact points to which they were attached. In order to capture the entire behaviour of the wallets and estimate the fracture energy in compression, the length of the vertical LVDTs were increased with respect to the one suggested by the standard. Two LVDTs (one for each side) were attached to the specimen to register the horizontal relative displacement over the length of the specimen. Their measuring range of every LVDT was 10 mm with an accuracy of 0.1%.

A 10-mm thick layer of gypsum was applied to faces in contact with the loading plates, to ensure that the loaded faces of the specimens were levelled and parallel to one another. This was done to prevent additional stresses in the specimens.

The specimens were tested using an apparatus provided with a 3000 kN hydraulic jack. The jack was positioned at the bottom. The hydraulic jack lifts a steel plate, the active side, and there was a passive load plate at the top. A hinge between the load cell and the top steel plate reduced possible eccentricities during loading. The hydraulic jack was operated in deformation control, using the displacement of the jack as control variable. A load cell that measures the applied force was attached to the top steel plate (Figure 3).

Three specimens were tested by applying a *monotonic loading* as prescribed by the EN 1052-1:1998 [11] (Figure 4). Half of the expected maximum compression force was applied in three equal steps and was kept constant for 2 ± 1 min. Afterwards, the maximum stress was reached monotonically. Subsequently, the test was continued to explore the post-peak behaviour. The load was applied with a rate of 0.003 mm/s to reach the peak stress in 15 to 30 min. The deformation and the force were registered, including the post-peak softening regime.

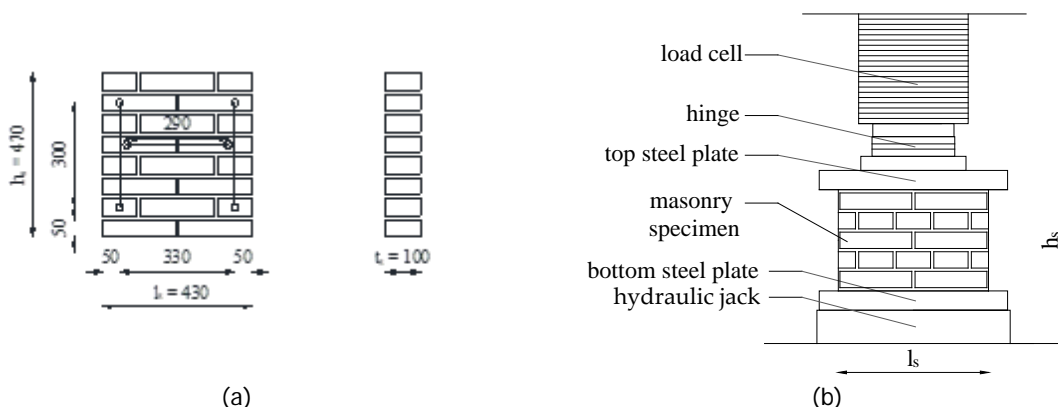


Figure 3 - Compression test on masonry wallets: (a) Dimensions of the clay single wythe specimens (TUD-MAT-31); (b) Test set-up used for compression test

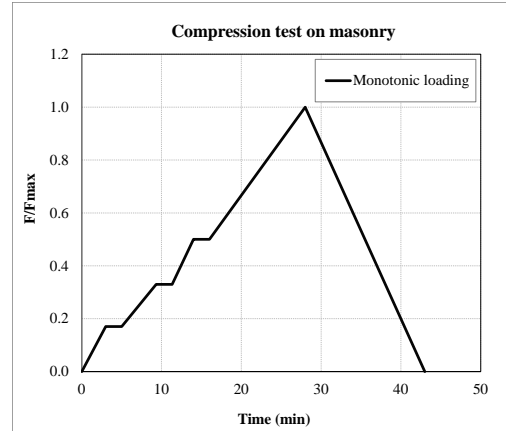


Figure 4 – Monotonic and cyclic loading scheme for compression test on masonry specimen.

6.2 Experimental results

Assuming that the stress is constant over the cross-section of the specimen, the compressive strength of masonry can be determined as follows:

$$f'_m = \frac{F_{max}}{t_s l_s} \quad (3)$$

where F_{max} is the maximum load, l_s , h_s and t_s are the dimensions of the masonry specimen as built (Figure 3a).

During the test the displacements and the force were measured continuously allowing the determination of the stress-strain relationship along the loading direction, which was defined as normal direction. From this relation was possible to determine the elastic modulus of masonry. Three estimates of the elastic modulus were adopted (Figure 5a):

- E_1 is the secant elastic modulus evaluated at 1/3 of the maximum stress;
- E_2 is the secant elastic modulus evaluated at 1/10 of the maximum stress;
- E_3 is the chord elastic modulus evaluated between 1/10 and 1/3 of the maximum stress.

The first estimate was consistent with the prescription of EN 1052-1:1998. The third estimate aimed to exclude the initial start-up of the stress-strain diagram, which would unrealistically affects the other two secant estimates with the initial lower slope.

The Poisson ratio ν is determined in the elastic phase as the ratio between the lateral strains, which are evaluated in the direction perpendicular to the loading one, and the normal strains (Figure 5 b).

The displacement control procedure of the test allowed determining the post-peak behaviour of the material. The fracture energy in compression $G_{f,c}$ was determined as the area underneath the normal stress versus normal strain diagram, taking the height of the specimen into account. This concept was introduced by van Mier [12] for concrete material and subsequently applied to masonry by Lourenco [13].

The strain obtained by LVDTs' readings and by the jack's readings resulted similar in the post-peak phase. Consequently, the former were used to evaluate the pre-peak phase, while the latter were used to describe the post-peak phase, in which LVDTs may be detached from the specimen due to extensive cracking. The elastic modulus and the Poisson ratio were calculated on the basis of the LVDTs readings, while the fracture energy was calculated on the basis of the LVDTs' reading in the pre-peak and jack's reading in the post-peak phase.

The strain associated with peak strength, which is called peak strain ϵ_p is reported in the current document.

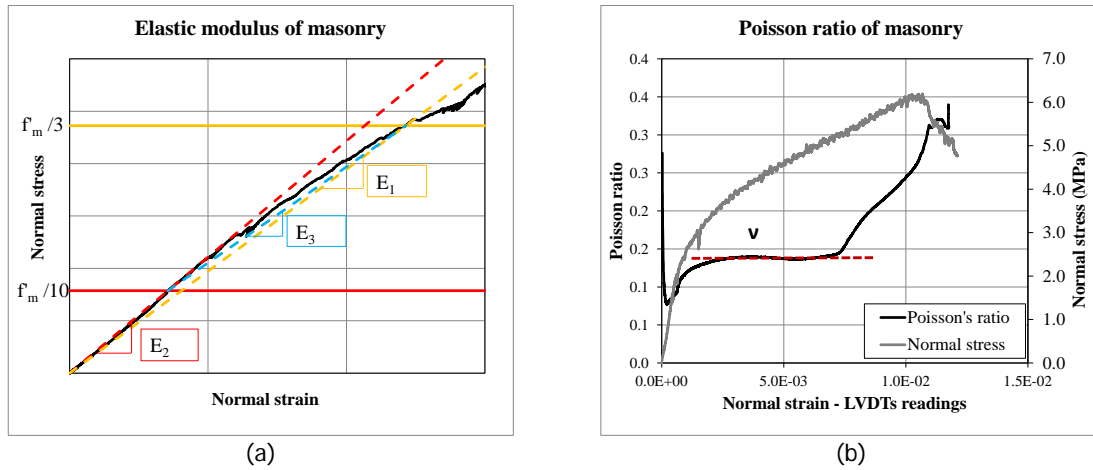


Figure 5 – Compression test on masonry: (a) three estimates of the elastic modulus; (b) evaluation of Poisson ratio.

Figure 6 and Figure 7 show the stress-strain diagram for the solid clay brick masonry for the construction period march 2019 and May 2019, respectively. The graphs refer to the normal direction that is defined as the one parallel to the loading direction.

The pre-peak stage was characterised by linear-elastic followed by a hardening behaviour until the peak. The nonlinearity started at approximately 1/3 of peak stress. After the peak stress was reached, an exponential softening behaviour was observed.

Figure 8 and Figure 9 analyses the development of cracks in the specimen tested under vertical compression test. In both cases, splitting cracks started in the bricks (Figure 8a and Figure 9a). Cracks mainly occurred in the central part of the specimens (Figure 8b and Figure 9b).

In the post-peak phase, the vertical cracks mainly occurred along the thickness of the specimens, by splitting it in two parts (Figure 8d, Figure 9d). The cracking was observed to occur in a distributed manner over the height of the specimen; no localisation of the cracking at the boundary was observed.

Table 8 and Table 9 list the main experimental results and Figure 10 and Figure 11 show the results in terms of the histogram representation. The tests were performed at 84 and 98 days hardening time for the specimen built in March 2019 and May 2019, respectively.

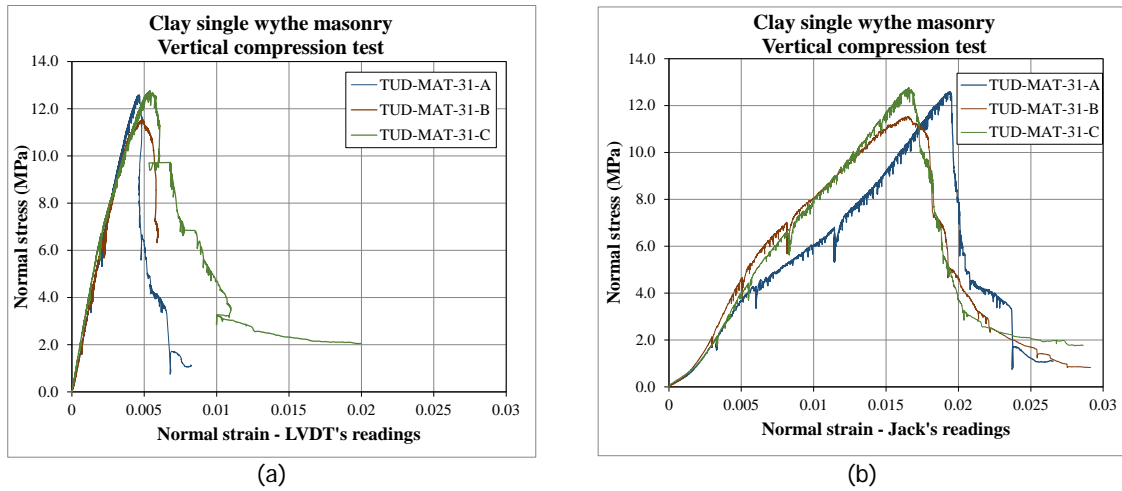


Figure 6 – Vertical compression tests construction period March 2019: (a) normal strain obtained by LVDT's reading; (b) normal strain obtained by jack's reading.

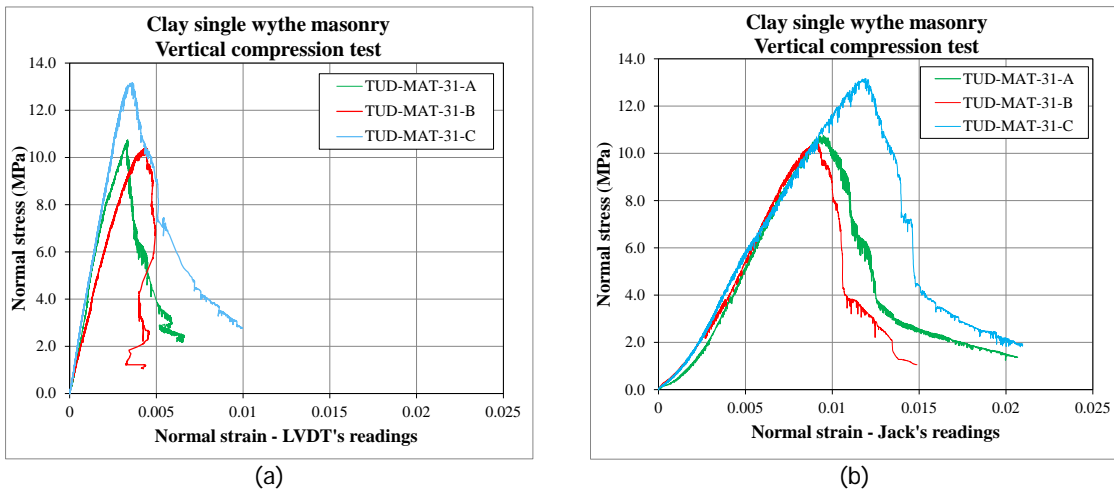


Figure 7 – Vertical compression tests construction period May 2019: (a) normal strain obtained by LVDT's reading; (b) normal strain obtained by jack's reading.

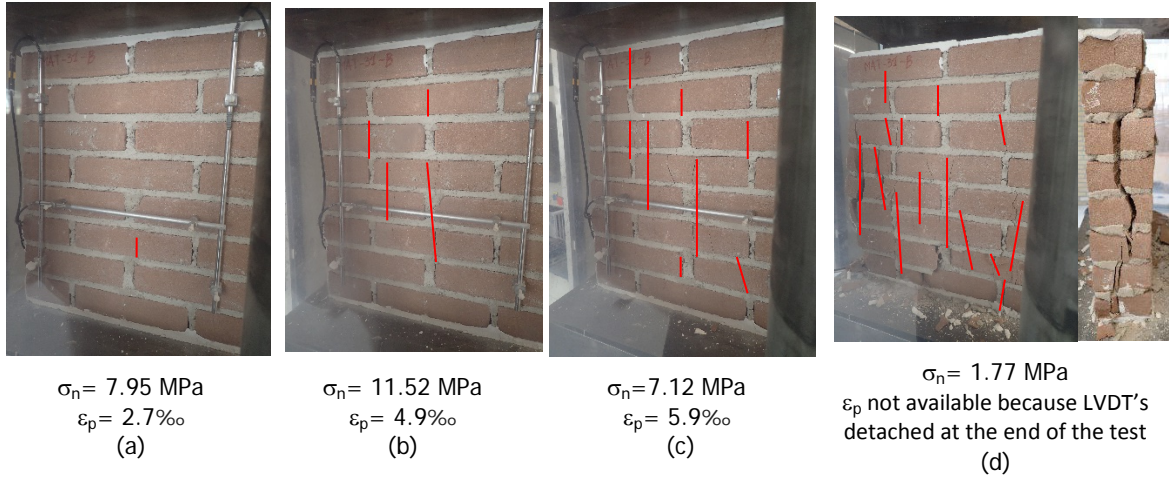


Figure 8 – Crack pattern of specimen TUD-MAT-31-C of construction period March 2019 tested under vertical compression: (a) first crack; (b) maximum stress; (c)-(d) post-peak phase.

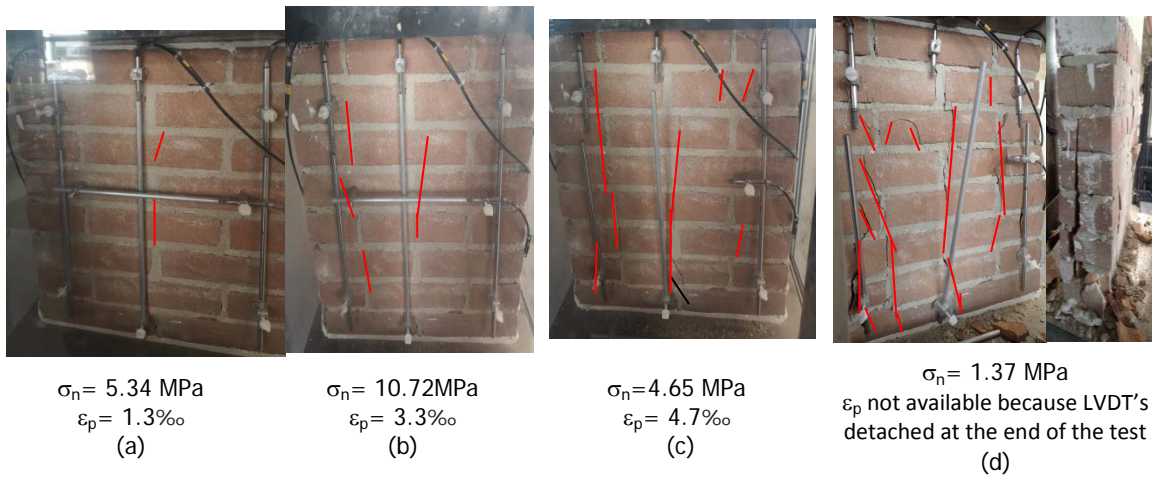


Figure 9 – Crack pattern of specimen TUD-MAT-31-A of construction period of May 2019 tested under vertical compression: (a) first crack; (b) maximum stress; (c)-(d) post-peak phase.

Table 8 – Vertical compression test results of clay single wythe masonry specimens built in March 2019.

Specimen name	Test type	f'_m	E_1	E_2	E_3	ϵ_p	G_{F-C}	ν
		MPa	MPa	MPa	MPa	‰	N/mm	
TUD_MAT-31A	monotonic	12.59	2485	2699	2391	4.5	24.45	0.14
TUD_MAT-31B	monotonic	11.53	3027	2685	3234	4.9	35.45	0.17
TUD_MAT-31C	monotonic	12.76	3503	3537	3486	5.4	35.21	0.21
Average		12.29	3005	2974	3037	4.9	31.70	0.17
Standard deviation		0.67	509	488	573	0.5	6.28	0.04
Coefficient of variation		0.05	0.17	0.16	0.19	0.09	0.20	0.20

Table 9 - Vertical compression test results of clay single wythe masonry specimens built in May 2019

Specimen name	Test type	f'_m	E_1	E_2	E_3	ϵ_p	G_{F-C}	ν
		MPa	MPa	MPa	MPa	‰	N/mm	-
TUD_MAT-31A	monotonic	10.76	3665	3264	3906	3.30	25.46	0.12
TUD_MAT-31B	monotonic	10.41	2943	3149	2850	4.30	22.16	0.16
TUD_MAT-31C	monotonic	13.17	4388	4332	4416	3.60	29.45	0.14
Average		11.45	3665	3582	3724	3.73	25.69	0.14
Standard deviation		1.50	723	652	799	0.51	3.65	0.02
Coefficient of variation		0.13	0.20	0.18	0.21	0.14	0.14	0.14

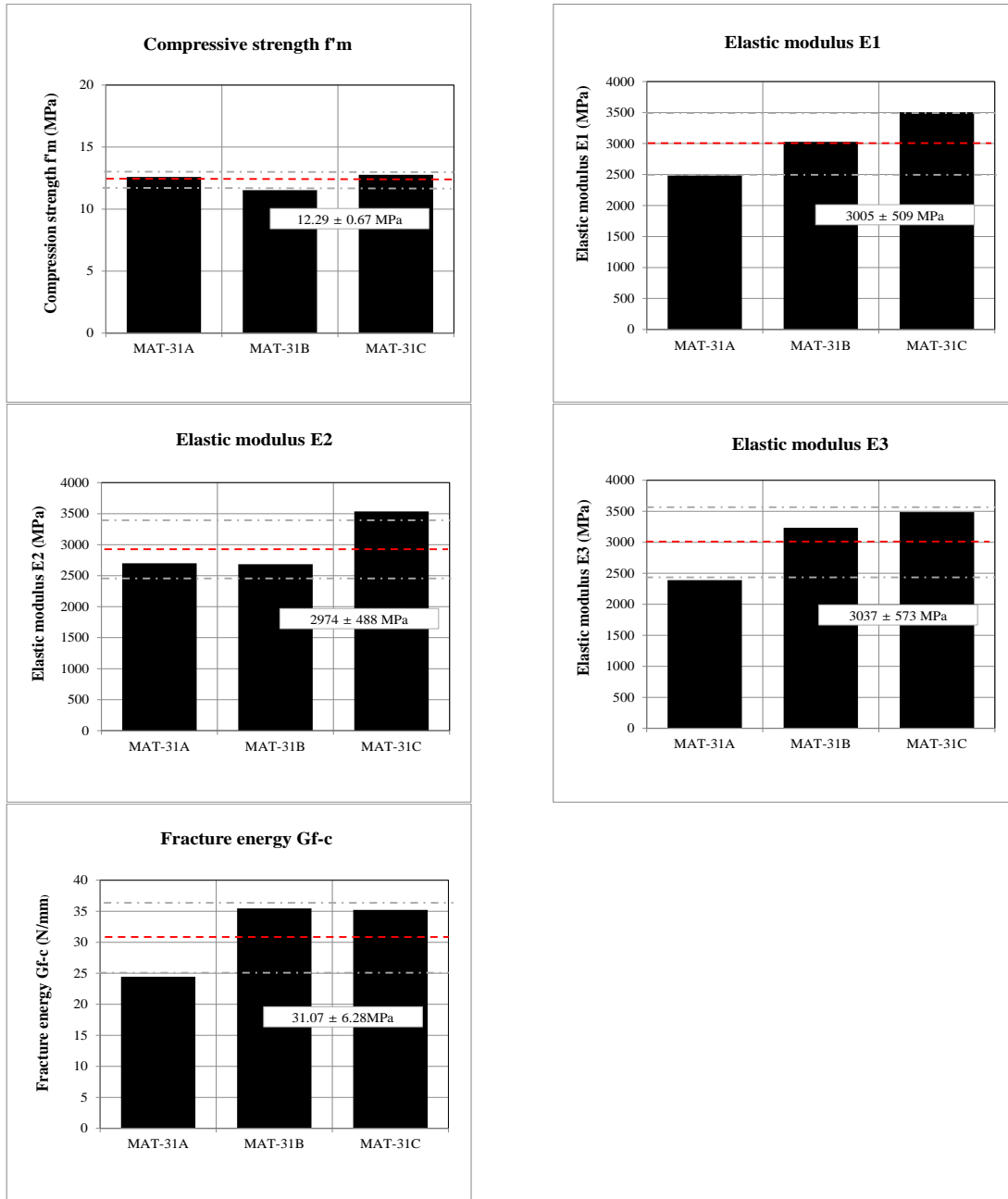


Figure 10– Vertical compression tests: histogram representation.

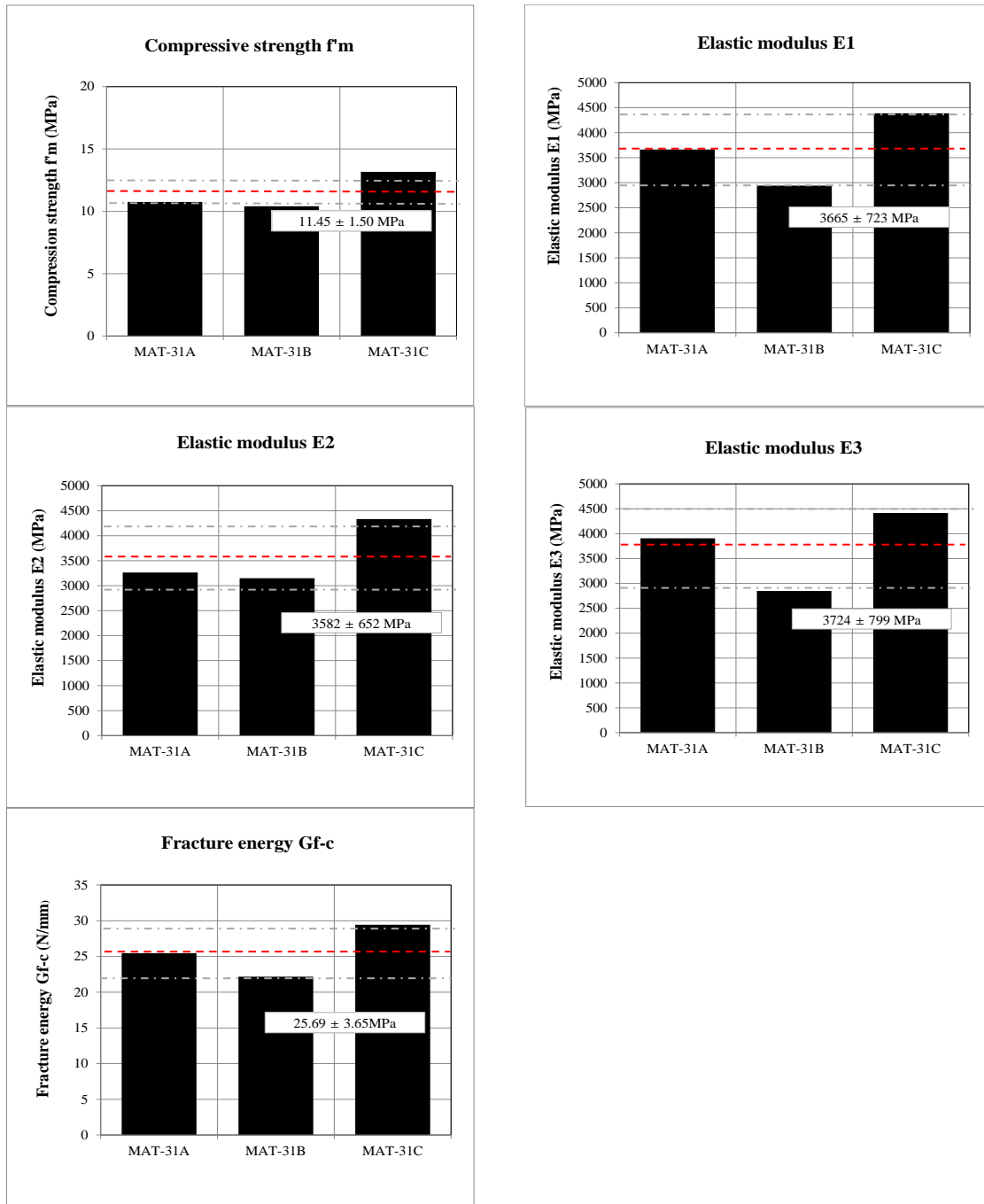


Figure 11 - Vertical compression tests construction period May 2019: histogram representation.

7 Bond strength of masonry

The bond strength between masonry unit and mortar was determined in agreement with the bond wrench test proposed by EN 1052-5:2005[14].

7.1 Testing procedure

Two different test set-up were used: manually controlled for the specimens of the construction period March 2019 and computer controlled for the specimens of the construction period May 2019.

The manually controlled test set-up used is shown in Figure 12a. The specimen was rigidly held by a support frame in accordance with EN 1052-5:2005 [14]. A clamp, with a lever attached, was applied to the upper part of the masonry unit. The lever was used to apply a bending moment to the brick-mortar interface. The load was manually controlled by measuring the torque applied; the value is showed on the screen of the lever.

In order to measure the post-peak softening response, the bond wrench set-up was recently improved using a computer-controlled apparatus. The same clamping system was used in the two cases. The apparatus had a hydraulic jack of 100kN capacity. The bed joint opening was monitored by two vertical LDVTS that were glued on the top steel clamp of the bond-wrench apparatus. Consequently, the measured displacement can be considered as a crack mouth opening displacement (CMOD). The LVDTs have a measuring range of 2 mm and an accuracy of 0.1%. The load was applied by controlling the CMOD and with a rate of 0.002 mm/s.

Twenty-one couplet specimens were adopted for the bond wrench tests of the construction period March 2019 and twenty-three for the construction period May 2019 (Figure 12c).

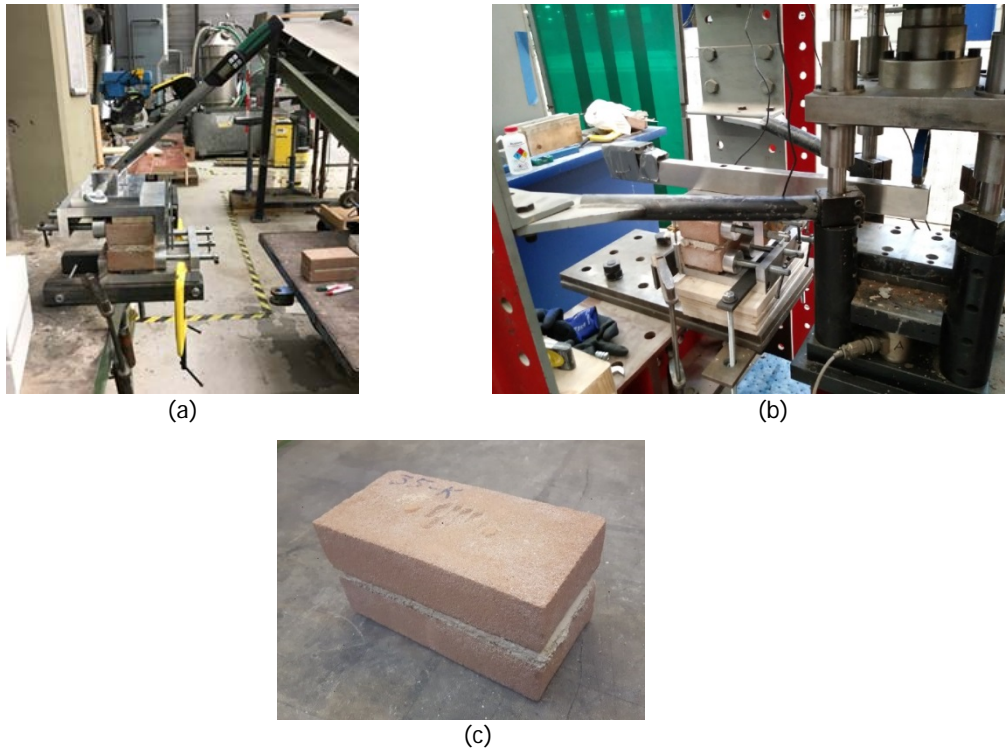


Figure 12 – Bond wrench tests: (a) manually controlled set-up; (b) computer controlled set-up; (c) couplet specimen.

7.2 Experimental results

The bond wrench strength f_w is calculated on the assumption that the stress distribution is linear over the width of the top masonry unit [14]:

$$f_w = \frac{F_1 e_1 + F_2 e_2 - \frac{2}{3} t_u \left(F_1 + F_2 + \frac{F_3}{4} \right)}{l_j w_j^2 / 6} \tag{4}$$

where F_1 is the failure load, measured and manually applied, F_2 is the normal force as a result of the weight of the bond wrench apparatus, F_3 is the weight of the masonry unit pulled off the specimen, including the weight of adherent mortar. Furthermore, e_1 is the distance from the applied load to the tension face of the specimen, e_2 is the distance from the centre of gravity of the clamp to the tension face of the specimen, l_j is the mean length of the bed joint, and w_j is the mean width of the bed joint. Figure 13 shows the set-up and the definition of the various quantities.

The computer controlled system allowed to determine the tension softening response of masonry [15]. To calculate the fracture energy G_{rw} , the area underneath the force versus the vertical jack displacement curve was considered as dissipated energy, and the cross-section of the tested interface was considered as the fracture surface.

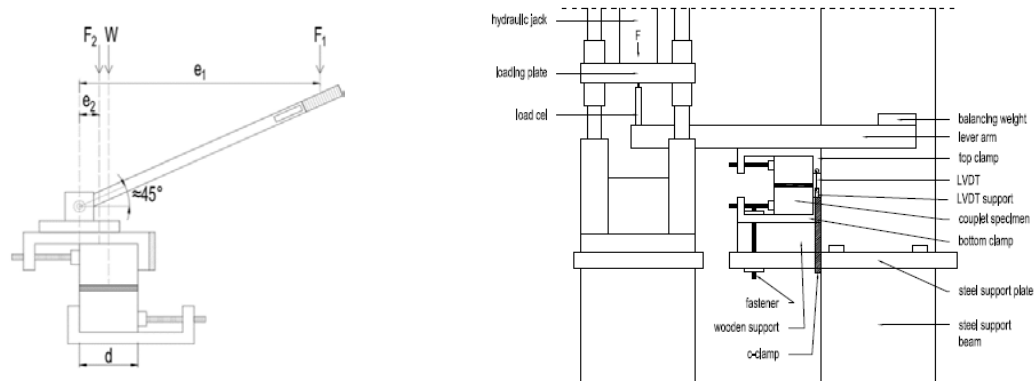


Figure 13 – Test set-up for the bond wrench test: (a) manually controlled; (b) computer controlled.

Figure 14 reports the classification of the type of failures [14], while Figure 15 shows the observed failure mechanisms.

In the construction period March 2019 the specimen were tested at 83 days of hardening time, while for the specimens built in May 2019 tests were carried out at 28 and 60 days. For the construction period March 2019, 14 over 21 specimens were de-bonded prior to testing, while for the construction period May 2019, 3 over 23 specimens were de-bonded.

Table 10 and Table 11 list the results of the bond wrench tests on solid clay brick masonry for both construction periods, including the average value weighted against all the specimens and the one including only the non-de-bonded samples. The bond strength values of specimens in terms of histogram are shown in Figure 16 and Figure 17. The bond wrench strength f_w results similar between the two construction periods. This indicates that the set-up adopted does not have an influence on the outcome of the test. Due to the similarity in failure mode, a comparison can be made between the bond wrench test and the out-of-plane bending test on wallets that generates a plane of failure parallel to the bed joints (OOP1). The out-of-plane bending test provided a value of fracture energy equal to $G_{fx1} = 0.0042 \pm 0.0019$ N/mm [2]. The values of fracture energy obtained with the computer controlled bond wrench set-up results higher, but they show also a large coefficient of variation (90%). The lower bound value ($0.022-0.020=0.002$ N/mm) is comparable with the one obtained with the out-of-plane flexural tests.

Figure 18 shows the force versus the displacement for solid clay brick masonry considering both the LVDTs and the Jack's reading. The continuous line refers to the specimens tested after 28 days and the dotted line to the ones tested after 60 days. Some specimens have a brittle failure after the peak and for other it is possible to record the post-peak.

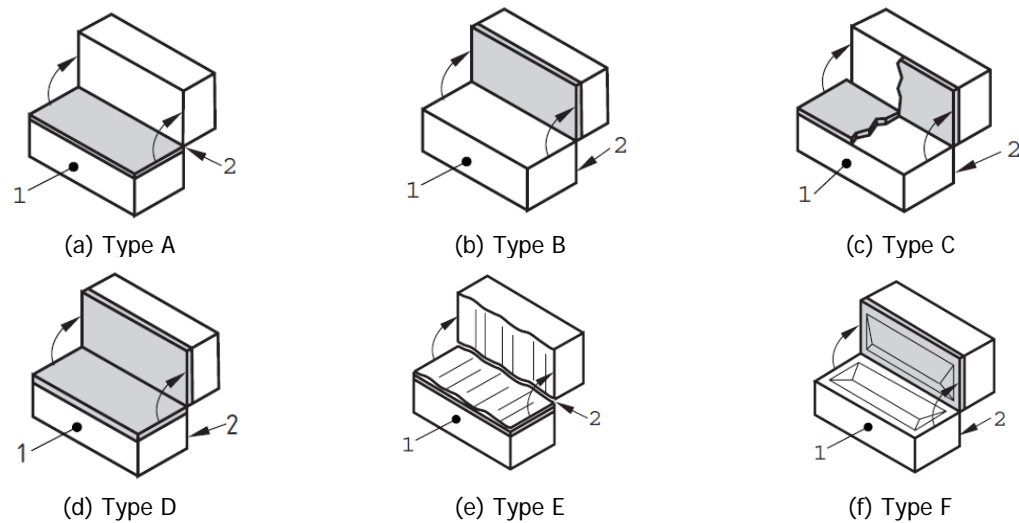


Figure 14 – Classification of failure modes in agreement with EN-1052-5:2005 (1 tension face, 2 compression face).



Figure 15 – Observed failure mechanisms: (a) type A; (b) type B.

Table 10 – Flexural bond strength construction period March 2019.

Specimen Name	l_j	w_j	F_3	T	f_w	Failure mode
	mm	mm	N	Nm	MPa	
TUD-MAT-35-A	209	100	15.84	43.80	0.10	A
TUD-MAT-35-B	207	100	16.67	0	0	-
TUD-MAT-35-C	210	100	16.67	0	0	-
TUD-MAT-35-D	210	100	15.98	39.60	0.09	A
TUD-MAT-35-E	208	100	16.67	0	0	-
TUD-MAT-35-F	206	100	20.59	52.40	0.12	B
TUD-MAT-35-G	207	100	16.38	0	0	-
TUD-MAT-35-H	210	100	16.33	45.10	0.10	A
TUD-MAT-35-I	211	100	16.67	0	0	-
TUD-MAT-35-L	212	100	16.67	0	0	-
TUD-MAT-35-M	209	100	16.67	0	0	-
TUD-MAT-35-N	205	100	16.03	0	0	-
TUD-MAT-35-O	207	100	16.67	0	0	-
TUD-MAT-35-P	210	100	16.28	14.4	0.10	A
TUD-MAT-35-Q	209	100	16.28	0	0	-
TUD-MAT-35-R	210	100	16.67	0	0	-
TUD-MAT-35-S	210	100	16.18	55.8	0.13	A
TUD-MAT-35-T	210	100	16.08	71.5	0.16	A
TUD-MAT-35-U	210	100	16.67	0	0	-
TUD-MAT-35-V	210	100	16.67	0	0	-
TUD-MAT-35-Z	207	100	16.67	0	0	-
Average considering only non-de-bonded specimens					0.10	
Standard deviation					0.04	
Coefficient of variation					0.42	
Average considering all the samples					0.04	
Standard deviation					0.05	
Coefficient of variation					1.46	

Table 11 - Flexural bond strength construction period May 2019.

Specimen Name	l_j	w_j	F_3	f_w	G_{rw}	Failure mode
	mm	mm	N	MPa	N/mm	
TUD-MAT-35-A	207	100	-	-	-	-
TUD-MAT-35-B	206	101	232.31	0.26	0.069	A
TUD-MAT-35-C	205	100	190.49	0.21	0.047	A
TUD-MAT-35-D	204	100	193.37	0.22	0.053	A
TUD-MAT-35-E	204	100	-	-	-	-
TUD-MAT-35-F	205	100	-	-	-	-
TUD-MAT-35-G	207	100	85.16	0.09	0.022	A
TUD-MAT-35-H	207	100	106.07	0.12	0.016	A
TUD-MAT-35-I	205	100	146.85	0.16	0.038	A
TUD-MAT-35-L	205	100	33.16	0.03	0.002	A
TUD-MAT-35-M	207	100	154.71	0.17	0.035	A
TUD-MAT-35-N	207	102	48.87	0.05	0.003	A
TUD-MAT-35-O	207	100	133.41	0.15	0.023	A
TUD-MAT-35-P	205	100	141.07	0.16	0.015	A
TUD-MAT-35-Q	204	100	39.21	0.04	0.002	A
TUD-MAT-35-R	207	102	21.60	0.02	0.001	A
TUD-MAT-35-S	206	100	159.11	0.18	0.043	A
TUD-MAT-35-T	206	102	133.16	0.14	0.028	A
TUD-MAT-35-U	207	100	38.06	0.04	0.002	A
TUD-MAT-35-V	208	102	38.18	0.04	0.003	A
TUD-MAT-35-W	205	100	172.09	0.19	0.025	A
TUD-MAT-35-X	206	100	72.36	0.08	0.007	B
TUD-MAT-35-Y	205	101	74.32	0.08	0.008	A
Average considering only non-de-bonded specimens				0.12	0.022	
Standard deviation				0.07	0.020	
Coefficient of variation				0.60	0.90	
Average considering all the samples				0.11	0.019	
Standard deviation				0.08	0.020	
Coefficient of variation				0.75	1.044	

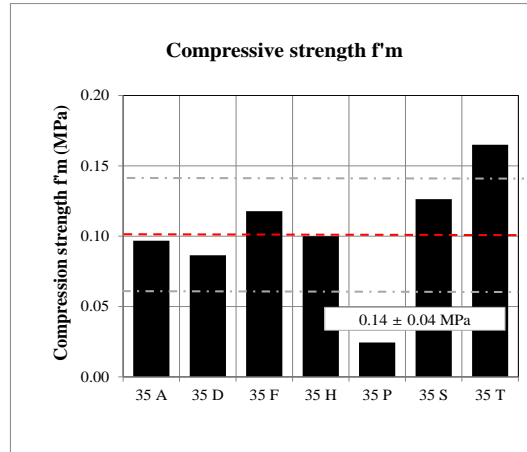


Figure 16 – Flexural bond strength values construction period March 2019: histogram representation.

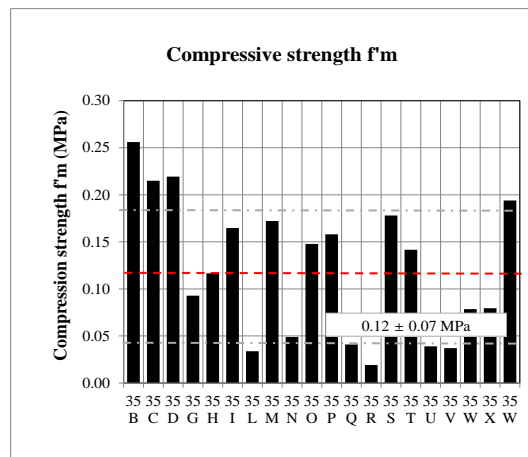


Figure 17 - Flexural bond strength values construction period May 2019: histogram representation.

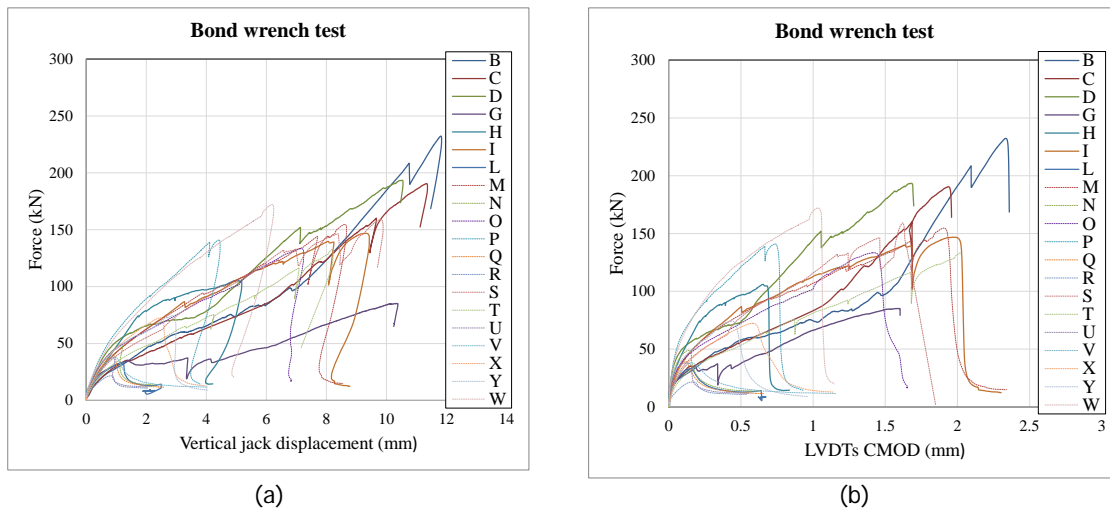


Figure 18 – Bond wrench test construction period May 2019: (a) Force versus vertical jack displacement; (b) force versus CMOD. Dashed and continuous lines refer to specimen tested after 28 and 60 days, respectively.

8 Shear strength of masonry

The initial shear properties of masonry were determined in agreement with EN 1052-3:2002 [16]. However, a displacement control procedure was used, instead of the prescribed force control procedure, to evaluate the residual strength properties and the mode-II fracture energy.

8.1 Testing procedure

The triplet is a three stacked bonded brick specimen (Figure 19). Nine specimens for each construction period were tested and prior to testing, a layer of gypsum was applied to the external faces of the specimens.

Figure 19 shows the test set-up used. During the test, the specimen was rotated of 90 degrees with respect to the casting position. The specimen was kept under constant lateral pre-compression, while a shear load was applied at the mid masonry unit. Three different levels of pre-compression were investigated. Being the compressive strength of the masonry unit greater than 10 N/mm^2 [16], the pre-compression stresses applied were 0.2, 0.6 and 1.0 N/mm^2 . For each pre-compression level, three specimens were tested.

Two independently operated jacks were required to apply the shear and pre-compressive load. The shear load acted in a vertical direction using a displacement controlled apparatus. The apparatus had a 100 kN jack and a spherical joint. The displacement increased with a rate of 0.005 mm/s . During unloading, the displacement was decreased with a rate of 0.05 mm/s . The pre-compressive load was applied perpendicular to the bed joint plane by a manually operated hydraulic jack. The horizontal hydraulic jack was used in force control. The jack was kept in position by means of four steel rods positioned on opposite sides of the specimen, which were in turn kept in position by steel plates (Figure 19a). In order to keep the transverse compressive load constant ($\pm 2\%$), a spring system was used between the hydraulic jack and the load cell. The stiffness of the springs was defined on the basis of the required pre-compression level and was equal to 123 N/mm and 3300 N/mm when the pre-compression stress was 0.2 and 0.6 or 1 N/mm^2 , respectively. A load cell was placed between the spring and the steel plate to measure the applied load.

Both on the front and the back side of the specimens, LVDTs were attached. Vertical LVDTs measured the relative vertical displacement of the middle brick with respect to the later ones. Horizontal LVDTs measured the horizontal displacement between the two external bricks. Their measuring range was 10 mm with an accuracy of 0.1% (Figure 19b).

To get more information regarding the post-peak behaviour, a second phase of the test was performed in which the pre-compression load was increased and kept constant in the residual phases. Due to the similarity of the results with previous experimental campaign ([2]-[4]), this procedure was adopted only for the specimen built in March 2019, for the second construction period (May 2019) a standard testing procedure (obtaining only one residual strength value in each test) was adopted.

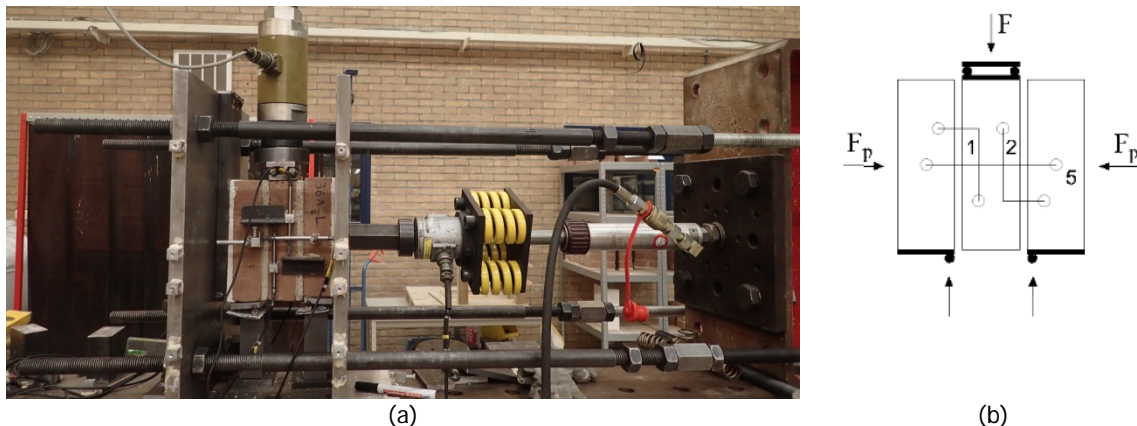


Figure 19 – (a) Test set-up for the shear-compression test; (b) LVDTs position.

8.2 Experimental results

The shear strength f_v was calculated for each specimen as follows [16]:

$$f_v = \frac{F_{\max}}{2A_s} \quad (5)$$

where F_{\max} is the maximum load, A_s is the cross sectional area of the specimen parallel to the bed joints. The pre-compression stress f_p can be calculated for each specimen as follows [16]:

$$f_p = \frac{F_p}{A_s} \quad (6)$$

where F_p is the pre-compression force.

The test was carried out in displacement control allowing for the determination of the post-peak behaviour. As a consequence, the residual shear strength $f_{v,res}$ was also determined. The residual strength occurred at an almost constant load where a plateau of large sliding displacement was observed. The resistance in the post-peak phase can be associated to friction only.

By adopting Coulomb friction law, all the results were plotted in a pre-compressive stress versus shear strength diagram. Considering a linear regression of the data, the initial shear strength f_{v0} and the initial coefficient of friction μ can be found such as the intercept with the vertical axis and the gradient of the line, respectively. The angle of internal friction α was determined as the angle between the regression line and the horizontal axis.

Similar consideration can be applied to determine the residual shear strength $f_{v0,res}$ and the residual coefficient of friction μ_{res} . In the Coulomb friction formulation, the result is:

$$f_v = f_{v0} + \mu f_p \quad (7)$$

$$f_{v,res} = f_{v0,res} + \mu_{res} f_p \quad (8)$$

Table 12 and Table 13 list the results of shear-compression test on triplets. The specimens were tested between 60 and 64 days after the first casting period and between 48 and 59 days after the second casting period. Totally, nine samples were tested for each construction period. Due to the incorrect installation of the LVDTs, the fracture energy could not be determined for specimen TUD-MAT-36-A. Specimens TUD-MAT-36-H and TUD-MAT-36-G resulted de-bonded prior to testing, consequently only the residual shear properties could be determined. Figure 20 and Figure 21 show the shear stress versus relative displacement curve of the triplets for the construction period March 2019 and May 2019, respectively. With the exception of specimen TUD-MAT-36-E (Figure 20c), the cracking at the two mortar-joint interfaces occurred simultaneously. The sliding of the middle unit was measured both from the LVDTs' reading and from jack's reading. The measuring range of LVDTs was 10 mm with an accuracy of 0.1%, beyond this range only the jack's measurement can be used to determine the residual strength.

Table 12 - Maximum and residual shear strength and mode-II fracture energy obtained from shear-compression tests on triplets of construction period March 2019.

$f_p = 0.2$ MPa				$f_p = 0.6$ MPa				$f_p = 1.0$ MPa			
Specimen name ^(*)	f_v	$f_{v,res}$	G_{f-II}	Specimen name ^(*)	f_v	$f_{v,res}$	G_{f-II}	Specimen name ^(*)	f_v	$f_{v,res}$	G_{f-II}
	MPa	MPa	N/mm		MPa	MPa	N/mm		MPa	MPa	N/mm
36 - C	0.36	0.16	0.09	36 - B	0.64	0.56	0.07	36 - A	0.96	0.75	-
36 - F	0.27	0.17	0.08	36 - E	0.72	0.49	0.22	36 - D	0.93	0.78	0.20
36 - I	0.30	0.19	0.05	36 - H**	-	0.53	-	36 - G**	-	0.79	-
-	-	-	-	-	-	-	-	36 - L	0.93	0.75	0.08
Average	0.31	0.17	0.07	Average	0.68	0.53	0.15	Average	0.95	0.77	0.14
St. dev.	0.06	0.01	0.01	St. dev.	0.06	0.05	0.11	St. dev.	0.03	0.02	0.08
C.o.V.	0.20	0.07	0.17	C.o.V.	0.09	0.10	0.73	C.o.V.	0.03	0.02	0.59

(*) Complete specimen name starting with TUD_MAT-.
 (**) Sample was de-bonded prior testing. Test was performed to find the residual properties.

Table 13 - Maximum and residual shear strength and mode-II fracture energy obtained from shear-compression tests on triplets of construction period May 2019.

$f_p = 0.2$ MPa				$f_p = 0.6$ MPa				$f_p = 1.0$ MPa			
Specimen name ^(*)	f_v	$f_{v,res}$	G_{f-II}	Specimen name ^(*)	f_v	$f_{v,res}$	G_{f-II}	Specimen name ^(*)	f_v	$f_{v,res}$	G_{f-II}
	MPa	MPa	N/mm		MPa	MPa	N/mm		MPa	MPa	N/mm
36 - D	0.29	0.21	0.05	36 - C	0.62	0.48	0.14	36 - B	0.87	0.76	0.08
36 - H	0.33	0.19	0.06	36 - G	0.55	0.40	0.12	36 - F	0.97	0.77	0.20
36 - M	0.32	0.22	0.04	36 - L	0.47	0.42	0.06	36 - I	0.92	0.72	0.36
Average	0.31	0.20	0.05	Average	0.55	0.43	0.10	Average	0.92	0.75	0.21
St. dev.	0.02	0.01	0.01	St. dev.	0.08	0.04	0.04	St. dev.	0.05	0.03	0.08
C.o.V.	0.06	0.07	0.24	C.o.V.	0.14	0.10	0.42	C.o.V.	0.06	0.04	0.40

(*) Complete specimen name starting with TUD_MAT-.
 (**) Sample was de-bonded prior testing. Test was performed to find the residual properties.

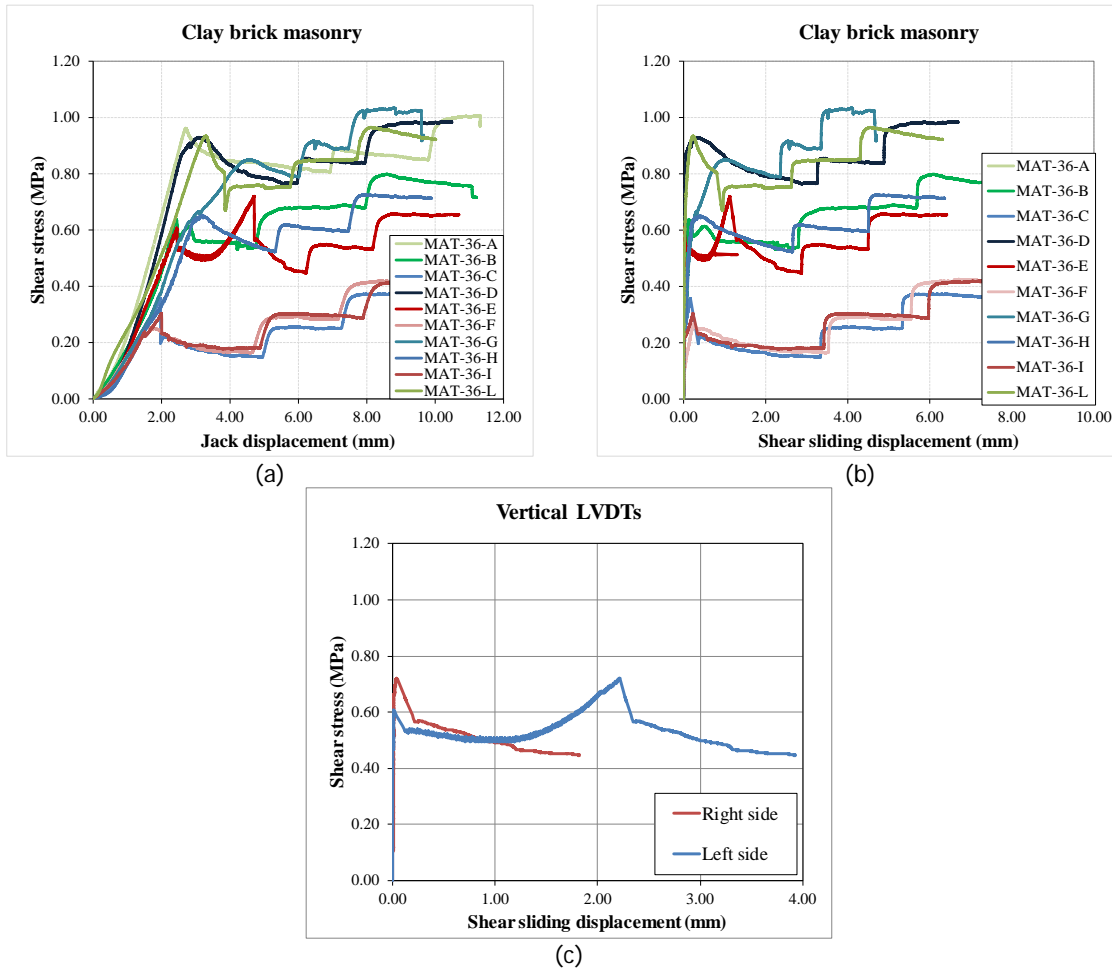


Figure 20 – Shear stress versus shear displacement construction period March 2019: (a) Considering the displacement of the jack; (b) Considering the relative displacement of the central brick from LVDTs' readings; (c) Detail of Figure 15b for specimen TUD-MAT-36-E.

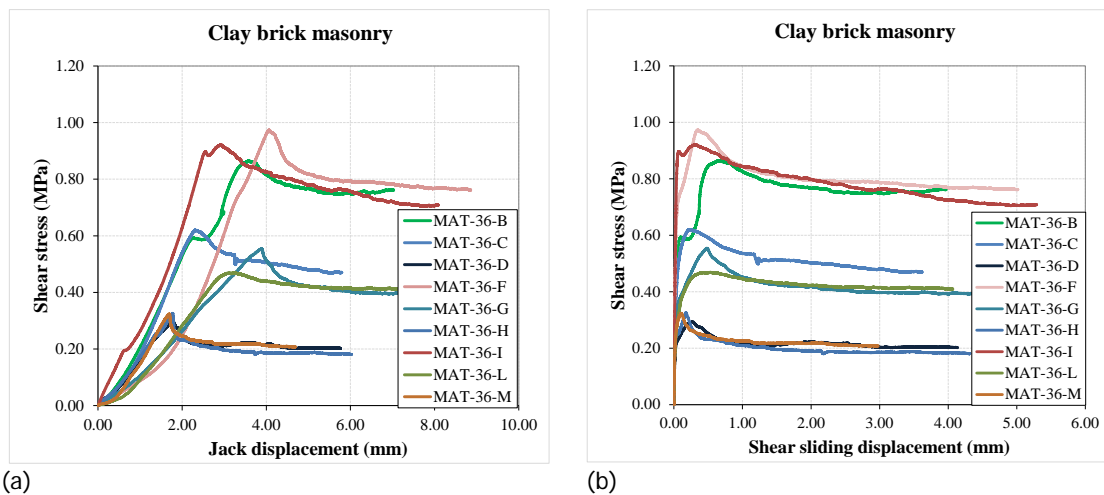


Figure 21 - Shear stress versus shear displacement construction period May 2019: (a) Considering the displacement of the jack; (b) Considering the relative displacement of the central brick from LVDTs' readings.

Figure 22 and Figure 23 show the results of the shear strength versus pre-compression stress for the two construction periods. No differences were observed for the specimens built in the two construction periods. A initial shear strength equal to 0.16 and 0.14 MPa was obtained for the specimen built in March 2019 and May 2019, respectively. A friction coefficient equal to 0.80 and 0.76 was obtained for the specimen built in the first and second construction, respectively. Figure 24 shows a typical crack pattern. Table 14 and Table 9 list a summary of the calculated shear properties.

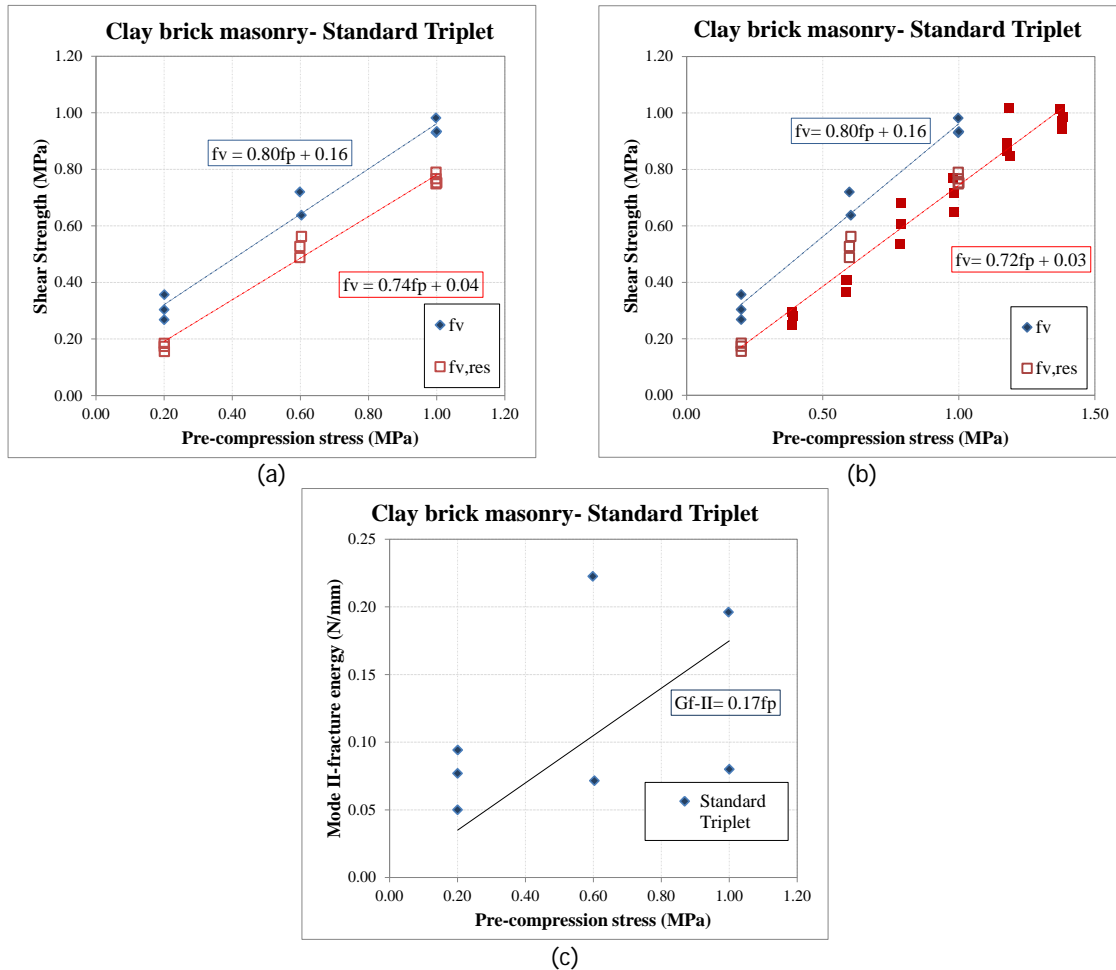


Figure 22 – Shear strength versus pre-compression stress for specimens built in March 2019: (a) data measured in the first phase; (b) data measured in the first and second phase of testing; (c) Mode II-fracture energy versus pre-compression.

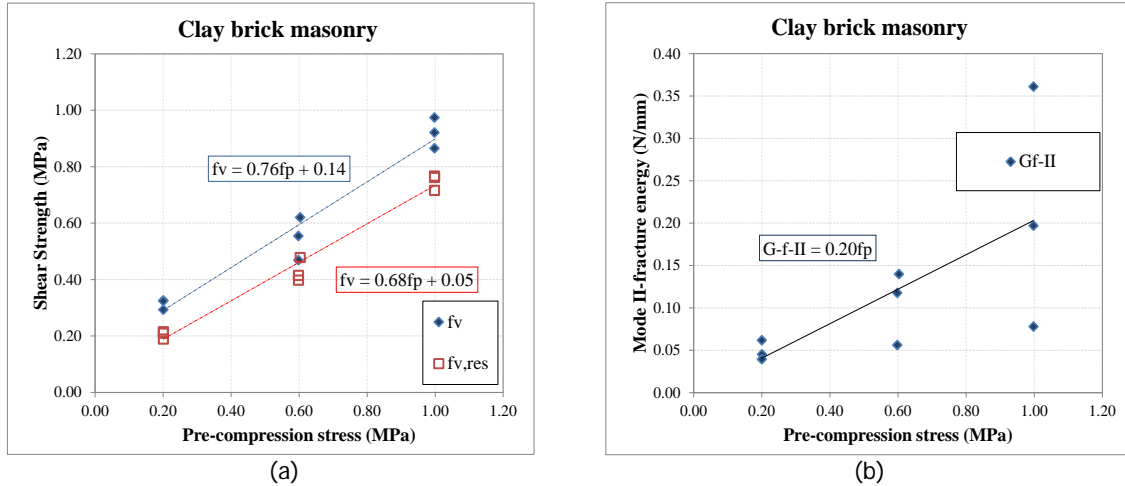


Figure 23 - Shear strength versus pre-compression stress for specimens built in May 2019: (a) data measured in the first phase; (b) Mode II-fracture energy versus pre-compression.

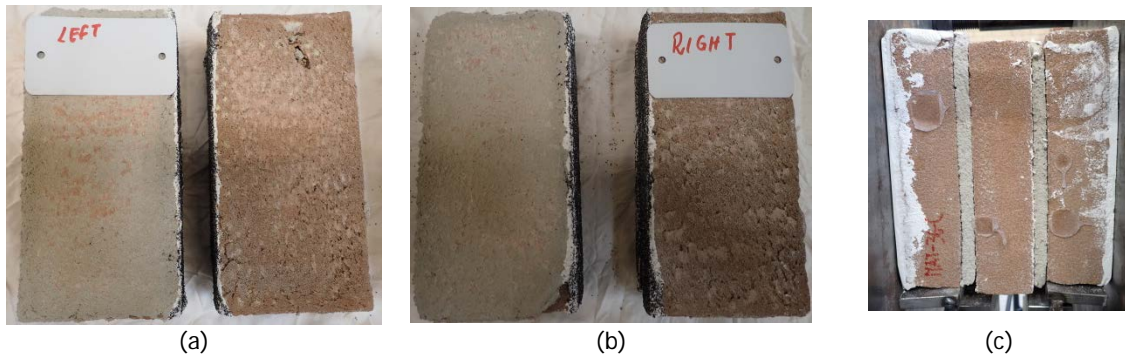


Figure 24 – Crack pattern of standard triplet under shear test: (a) front-left joint; (b) front-right joint; (c) front view.

Table 14 - Shear properties of solid clay brick masonry construction period March 2019.

Property	Symbol	Unit	Value
Number of specimens			9
Initial shear strength	f_{v0}	MPa	0.16
Initial coefficient of friction	μ		0.80
Angle of internal friction	α		38.65
Residual shear strength	$f_{res,v}$	MPa	0.03
Residual coefficient of friction	μ_{res}		0.72
Residual angle of internal friction	α_{res}		35.75

Table 15 - Shear properties of solid clay brick masonry construction period May 2019.

Property	Symbol	Unit	Value
Number of specimens			9
Initial shear strength	f_{v0}	MPa	0.14
Initial coefficient of friction	μ		0.76
Angle of internal friction	α		37.23
Residual shear strength	$f_{res,v}$	MPa	0.05
Residual coefficient of friction	μ_{res}		0.68
Residual angle of internal friction	α_{res}		34.21

9 Summary and properties overview

This report concerns with the characterisation of solid clay brick masonry at material level. These companion tests have been carried out in support to the testing campaign on connection between masonry walls and timber floor performed in WP2 [1]. The results can serve as input for analytical and numerical models of the tested connections.

The masonry was made of general purpose mortar and solid clay brick, these materials were frequently used for the construction of residential buildings in the Netherland. An extensive characterisation of the solid clay brick masonry was provided in a previous experimental campaign carried out in 2016 [2]; furthermore the same material was used in Ref. [3]-[4]. Consequently, only limited companion tests were performed in this case. The bricks and mortar used in this and previous experimental campaign belong to a single production batch; the same construction procedure has been adopted. The material was originally selected to replicate properties of solid clay brick masonry as obtained by tests on specimens extracted from existing buildings in Groningen [5]. A complete overview of this selection can be found in Ref. [6]. The experimental results presented in this document are in line with results from previous experimental campaigns.

An overview of the material properties of solid clay brick masonry is listed in Table 16 including the results presented in this report (construction period March 2019 and May 2019) and the one obtained in previous testing campaigns [2]-[4]. In this testing campaign only the compression, flexure and shear properties of masonry specimens were measured. The compression tests were performed in the direction perpendicular to the bed-joints. The flexure properties of the masonry were studied by performing bond wrench tests. A new computer-controlled bond wrench set-up was designed allowing also the determination of the fracture energy (in tension). The shear properties of masonry were obtained by performing shear tests on triplets. By adopting a displacement-controlled procedure, the initial shear parameters, including initial shear strength and coefficient of friction was studied and the residual strength property, where a plateau was reached, was investigated.

Table 16 – Overview of mechanical properties of solid clay brick.

Property	Symbol	Unit	Construction period October 2016 [2]				Construction period May 2017 [3]				Construction period July 2018 [4]				Standard
			Average	St. dev.	C.o.V.	No. test	Average	St. dev.	C.o.V.	No. test	Average	St. dev.	C.o.V.	No. test	
Compressive strength of mortar	f_m	MPa	3.81	0.34	0.09	108	3.84	0.43	0.11	108	3.59	0.34	0.09	12	EN 1015-11:1999
Flexural strength of mortar	f_{mt}	MPa	1.40	0.17	0.12	54	1.57	0.11	0.07	54	1.55	0.16	0.10	24	
Normalised compressive strength of masonry unit	f_b^*	MPa	28.31	2.92	0.10	9	-	-	-	-	-	-	-	-	EN 772-1:2000
Elastic modulus of masonry unit	E_b^*	MPa	8049	423	0.05	2	-	-	-	-	-	-	-	-	
Flexural strength of masonry unit	f_{bt}^*	MPa	6.31	0.72	0.11	8	-	-	-	-	-	-	-	-	EN 6790:2015
Density of masonry	ρ	kg/m ³	1708	71	0.04	19	-	-	-	-	-	-	-	-	-
Compressive strength of masonry in the direction perpendicular to bed joints	f_m	MPa	14.02	0.56	0.04	6	11.35	0.83	0.07	6	12.93	0.89	0.07	3	EN 1052-1:1998
Elastic modulus of masonry in the direction perpendicular to bed joints calculated at 1/3 of the maximum stress	E_1	MPa	4380	605	0.14		2919	442	0.15		3206	800	0.25		
Elastic modulus of masonry in the direction perpendicular to bed joints calculated at 1/10 of the maximum stress	E_2	MPa	4068	783	0.19		2731	732	0.27		3265	938	0.29		
Elastic modulus of masonry in the direction perpendicular to bed joints calculated between 1/3 and 1/10 of the maximum stress	E_3	MPa	4590	603	0.13		3087	315	0.10		3190	762	0.24		
Fracture energy in compression for loading perpendicular to bed joints	G_{fc}	N/mm	28.52	3.40	0.12		26.05	3.15	0.12		28.63	3.1	0.11		
Poisson ratio of masonry in compression for loading perpendicular to bed joints	ν	-	0.14	0.02	0.11		0.14	0.004	0.03		0.16	0.06	0.35		
Peak strain in compression for loading perpendicular to bed joints	ϵ_p	%	4.30	0.40	0.10	5.2	0.56	0.11	5.03	0.80	0.16				
Compressive strength of masonry in the direction parallel to bed joints	$f_{m,h}$	MPa	13.11	2.41	0.18	6	-	-	-	-	-	-	-	-	-
Elastic modulus of masonry in the direction parallel to bed joints calculated at 1/3 of the maximum stress	$E_{1,h}$	MPa	3332	565	0.17		-	-	-		-	-	-		
Elastic modulus of masonry in the direction parallel to bed joints calculated at 1/10 of the maximum stress	$E_{2,h}$	MPa	3664	689	0.19		-	-	-		-	-	-		
Elastic modulus of masonry in the direction parallel to bed joints calculated between 1/3 and 1/10 of the maximum stress	$E_{3,h}$	MPa	3207	592	0.18		-	-	-		-	-	-		
Fracture energy in compression for loading parallel to bed joints	$G_{fc,h}$	N/mm	35.06	6.63	0.19		-	-	-		-	-	-		
Peak strain in compression for loading parallel to bed joints	$\epsilon_{p,h}$	%	5.80	1.0	0.19		-	-	-		-	-	-		
Masonry flexural strength with the moment vector parallel to the bed joints and in the plane of the wall	f_{x1}	MPa	0.16	0.03	0.21	4	-	-	-	-	-	-	-	-	EN 1052-2:1999
Elastic modulus in bending with the moment vector parallel to the bed joints and in the plane of the wall	E_{fx1}	MPa	3756	365	0.10		-	-	-		-	-	-		
Fracture energy obtained from bending tests with the moment vector parallel to the bed joints and in the plane of the wall	G_{fx1}	N/mm	0.0042	0.002	0.45		-	-	-		-	-	-		
Masonry flexural strength with the moment vector orthogonal to the bed joint and in the plane of the wall	f_{x2}	MPa	0.65	0.19	0.28	5	-	-	-	-	-	-	-	-	EN 1052-2:1999
Elastic modulus in bending with the moment vector orthogonal to the bed joint and in the plane of the wall	E_{fx2}	MPa	7080	593	0.08		-	-	-		-	-	-		
Fracture energy obtained from bending tests with the moment vector orthogonal to the bed joints and in the plane of the wall	G_{fx2}	N/mm	0.17	0.09	0.52		-	-	-		-	-	-		
Masonry flexural strength with the moment vector orthogonal to the plane of the wall	f_{x3}	MPa	0.46	0.10	0.22	7	-	-	-	-	-	-	-	-	EN 1052-2:1999
Elastic modulus in bending with the moment vector orthogonal to the plane of the wall	E_{fx3}	MPa	2924	480	0.16		-	-	-		-	-	-		
Fracture energy obtained from bending tests with the moment vector orthogonal to the plane of the wall	G_{fx3}	N/mm	0.19	0.07	0.35		-	-	-		-	-	-		
Flexural bond strength	f_w	MPa	0.15	0.05	0.32	13	0.09	0.03	0.35	10	0.08	0.03	0.32	10	EN 1052-5:2002
Fracture energy obtained with computer controlled bond wrench test	G_{fw}	N/mm	-	-	-	-	-	-	-	-	0.12	0.011	0.860		
Masonry (bed joint) initial shear strength	f_{v0}	MPa	0.20	-	-	8	0.14	-	-	6	0.13	-	-	6	EN 1052-3:2002
Masonry (bed joint) shear friction coefficient	μ	-	0.69	-	-		0.79	-	-		0.82	-	-		
Residual masonry (bed joint) initial shear strength	$f_{v0,res}$	MPa	0.05	-	-		0.03	-	-		0.04	-	-		
Residual masonry (bed joint) shear friction coefficient	μ_{res}	-	0.60	-	-		0.71	-	-		0.63	-	-		

*the bricks belong to the same batch tested in 2016 [2].

Table 16 – Overview of mechanical properties of solid clay brick. (Cont.)

Property	Symbol	Unit	Construction period March 2019				Construction period May 2019				Standard
			Average	St. dev.	C.o.V.	No. test	Average	St. dev.	C.o.V.	No. test	
Compressive strength of mortar	f_m	MPa	4.65	0.42	0.09	12	5.04	0.67	0.13	12	EN 1015-11:1999
Flexural strength of mortar	f_{mf}	MPa	2.17	0.33	0.15	24	1.92	0.30	0.16	24	
Normalised compressive strength of masonry unit	f_b^*	MPa	-	-	-	-	-	-	-	-	EN 772-1:2000
Elastic modulus of masonry unit	E_p^*	MPa	-	-	-	-	-	-	-	-	
Flexural strength of masonry unit	f_{bt}^*	MPa	-	-	-	-	-	-	-	-	EN 6790:2015
Density of masonry	ρ	kg/m ³	1618	15	0.01	20	1586	15	0.09	23	-
Compressive strength of masonry in the direction perpendicular to bed joints	f_m	MPa	12.29	0.67	0.05	3	11.45	1.50	0.12	3	EN 1052-1:1998
Elastic modulus of masonry in the direction perpendicular to bed joints calculated at 1/3 of the maximum stress	E_1	MPa	3005	509	0.17		3665	723	0.20		
Elastic modulus of masonry in the direction perpendicular to bed joints calculated at 1/10 of the maximum stress	E_2	MPa	2974	488	0.16		3582	652	0.18		
Elastic modulus of masonry in the direction perpendicular to bed joints calculated between 1/3 and 1/10 of the maximum stress	E_3	MPa	3037	573	0.19		3724	799	0.21		
Fracture energy in compression for loading perpendicular to bed joints	$G_{f,c}$	N/mm	31.70	6.30	0.20		25.69	3.65	0.14		
Poisson ratio of masonry in compression for loading perpendicular to bed joints	ν	-	0.17	0.04	0.20		0.14	0.02	0.14		
Peak strain in compression for loading perpendicular to bed joints	ϵ_p	‰	4.90	0.50	0.09	3.73	0.51	0.14			
Compressive strength of masonry in the direction parallel to bed joints	$f_{m,h}$	MPa	-	-	-	-	-	-	-	-	-
Elastic modulus of masonry in the direction parallel to bed joints calculated at 1/3 of the maximum stress	$E_{1,h}$	MPa	-	-	-	-	-	-	-	-	
Elastic modulus of masonry in the direction parallel to bed joints calculated at 1/10 of the maximum stress	$E_{2,h}$	MPa	-	-	-	-	-	-	-	-	
Elastic modulus of masonry in the direction parallel to bed joints calculated between 1/3 and 1/10 of the maximum stress	$E_{3,h}$	MPa	-	-	-	-	-	-	-	-	
Fracture energy in compression for loading parallel to bed joints	$G_{f,c,h}$	N/mm	-	-	-	-	-	-	-	-	
Peak strain in compression for loading parallel to bed joints	$\epsilon_{p,h}$	‰	-	-	-	-	-	-	-	-	
Masonry flexural strength with the moment vector parallel to the bed joints and in the plane of the wall	f_{x1}	MPa	-	-	-	-	-	-	-	-	EN 1052-2:1999
Elastic modulus in bending with the moment vector parallel to the bed joints and in the plane of the wall	E_{fx1}	MPa	-	-	-	-	-	-	-	-	
Fracture energy obtained from bending tests with the moment vector parallel to the bed joints and in the plane of the wall	G_{fx1}	N/mm	-	-	-	-	-	-	-	-	
Masonry flexural strength with the moment vector orthogonal to the bed joint and in the plane of the wall	f_{x2}	MPa	-	-	-	-	-	-	-	-	EN 1052-2:1999
Elastic modulus in bending with the moment vector orthogonal to the bed joint and in the plane of the wall	E_{fx2}	MPa	-	-	-	-	-	-	-	-	
Fracture energy obtained from bending tests with the moment vector orthogonal to the bed joints and in the plane of the wall	G_{fx2}	N/mm	-	-	-	-	-	-	-	-	
Masonry flexural strength with the moment vector orthogonal to the plane of the wall	f_{x3}	MPa	-	-	-	-	-	-	-	-	EN 1052-2:1999
Elastic modulus in bending with the moment vector orthogonal to the plane of the wall	E_{fx3}	MPa	-	-	-	-	-	-	-	-	
Fracture energy obtained from bending tests with the moment vector orthogonal to the plane of the wall	G_{fx3}	N/mm	-	-	-	-	-	-	-	-	
Flexural bond strength	f_w	MPa	0.10	0.04	0.42	8	0.12	0.07	0.60	20	EN 1052-5:2002
Fracture energy obtained with computer controlled bond wrench test	G_{fw}	N/mm	-	-	-	-	0.022	0.020	0.90	-	-
Masonry (bed joint) initial shear strength	f_{v0}	MPa	0.16	-	-	9	0.14	-	-	9	EN 1052-3:2002
Masonry (bed joint) shear friction coefficient	μ	-	0.80	-	-		0.76	-	-		
Residual masonry (bed joint) initial shear strength	$f_{v0,res}$	MPa	0.03	-	-		-	-	-		
Residual masonry (bed joint) shear friction coefficient	μ_{res}	-	0.72	-	-		-	-	-		

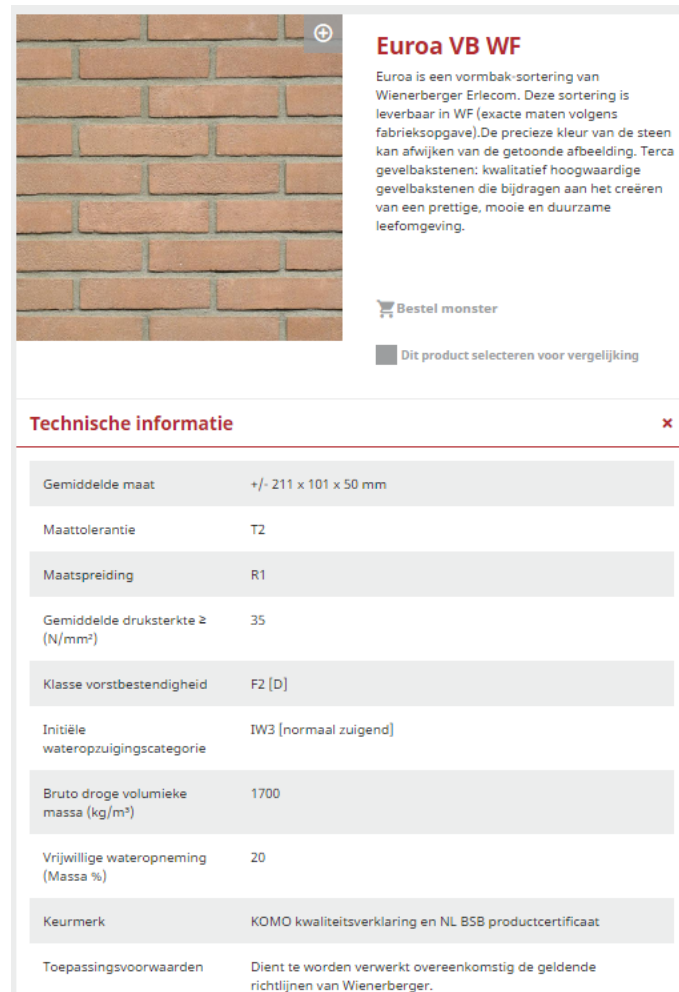
References

- [1] Mirra, M., Ravenshorst G. J. P. (2019). Monotonic, cyclic and dynamic behaviour of joist-masonry connections - Phase 1. Delft University of Technology. Report number CS2B04-WP2-3.1, version 1, 3 June 2019
- [2] Jafari S., Esposito R. (2017). Material tests for the characterisation of replicated solid clay brick masonry. Delft University of Technology. Report number C31B67WP1-12, version 01, 16 August 2017.
- [3] Korswagen P., Longo M., Meulman E., van Hoogdalem C. (2017). Damage sensitivity of Groningen masonry structures – experimental and computational studies. Delft University of Technology. Report number C31B69WPO-12, Version 1.2. 30 December 2017.
- [4] Korswagen P., Longo M., Meulman E., (2019). Damage sensitivity of Groningen masonry structures – experimental and computational studies. Delft University of Technology. Report number C31B69WPO-14-1, Version 1.1., 1 March 2019.
- [5] Jafari S., J.G. Rots and L. Panoutsopoulou, Tests for the characterization of original Groningen masonry, Delft University of Technology, Dept. Structural Engineering, 18 December 2015.
- [6] Esposito, R., Meulman, E., Jafari, S. and Ravenshorst, G. (2016). Quasi-static cyclic tests on masonry components. Delft University of Technology. Report number C31B67WP3-3, version 2, 13 December 2016.
- [7] EN 1996-1-1+A1 (2013). Eurocode 6 – Design of masonry structures – Part 1-1: General rules for reinforced and unreinforced masonry structures. Nederlands Normalisatie-instituut (NEN).
- [8] Protocol for the construction of masonry, ver. 18-03-2015.
- [9] EN 1015-3 (1999). Method of test for mortar for masonry – Part 3: Determination of consistence of fresh mortar (by flow table). Nederlands Normalisatie-instituut (NEN).
- [10] EN 1015-11 (1999). Method of test for mortar for masonry – Part 11: Determination of flexural strength of hardened mortar. Nederlands Normalisatie-instituut (NEN).
- [11] EN 1052-1 (1998). Method of test masonry – Part 1: Determination of compressive strength. Nederlands Normalisatie-instituut (NEN).
- [12] Van Mier, J.G.M (1984). Strain softening of concrete under multiaxial loading conditions, PhD thesis, Eindhoven University of Technology.
- [13] Lourenco, P.B., De Borst, R. and Rots, J.G. (1997). A plane stress softening plasticity model for orthotropic materials. International Journal for Numerical Methods in Engineering 40(21), 4033-4057.
- [14] EN 1052-5 (2005). Method of test masonry – Part 5: Determination of bond strength by bond wrench method. Nederlands Normalisatie-instituut (NEN).
- [15] Pluijm R. Out-of-plane bending of masonry behaviour and strength: Technische Universiteit Eindhoven; 1999.
- [16] EN 1052-3 (2002). Method of test masonry – Part 3: Determination of initial shear strength. Nederlands Normalisatie-instituut (NEN).
- [17] EN 1052-2 (1999). Method of test masonry – Part 2: Determination of flexural strength. Nederlands Normalisatie-instituut (NEN).

Appendix A

This appendix reports information on the brick and mortar used for the clay brick masonry as given by the producers. Table A.1 lists the characteristics of the clay bricks Euroa VB WF produced by Wienerberger. Table A.2 lists the composition of mortar BM2 version 2, having cement:lime:sand proportions equal to 1:2:9, produced by Remix.

Table A.1 – Declaration of performance of clay bricks (<http://wienerberger.nl/producten/euroa-vb#collapse-collapse1366232660485>, 28 July 2017).



Euroa VB WF

Euroa is een vormbak-sortering van Wienerberger Erlecom. Deze sortering is leverbaar in WF (exacte maten volgens fabrieksopgave). De precieze kleur van de steen kan afwijken van de getoonde afbeelding. Terca gevelbakstenen: kwalitatief hoogwaardige gevelbakstenen die bijdragen aan het creëren van een prettige, mooie en duurzame leefomgeving.

[Bestel monster](#)

Dit product selecteren voor vergelijking

Technische informatie ✕

Gemiddelde maat	+/- 211 x 101 x 50 mm
Maattolerantie	T2
Maatspreiding	R1
Gemiddelde druksterkte \geq (N/mm ²)	35
Klasse vorstbestendigheid	F2 [D]
Initiële wateropzuigingscategorie	IW3 [normaal zuigend]
Bruto droge volumieke massa (kg/m ³)	1700
Vrijwillige wateropneming (Massa %)	20
Keurmerk	KOMO kwaliteitsverklaring en NL BSB productcertificaat
Toepassingsvoorwaarden	Dient te worden verwerkt overeenkomstig de geldende richtlijnen van Wienerberger.

Table A.2 – Composition of clay brick masonry mortar BM2 version 2 (Personal communication, 25 July 2016)

Raw material	Unit	Quantity
Cement CEM1 42.5R	kg	60
Limestone filler 0.09 mm	kg	40
Hydrated lime CL80S	kg	90
Sand (0.00-1.20 mm)	kg	630
Sand (1.20-3.55 mm)	kg	180
air entrained	kg	0.05